# Fundamental constraints on broadband passive acoustic treatments in unidimensional scattering problems

Yang Meng, Vicente Romero-García, Gwénaël Gabard, Jean-Philippe Groby, Charlie Bricault, Sébastien Goudé, Ping Sheng

# Fundamental constraints on broadband passive acoustic treatments in unidimensional scattering problems

Yang Meng, Vicente Romero-García, Gwénaël Gabard, and Jean-Philippe Groby

*Laboratoire d'Acoustique de l'Université du Mans (LAUM),*

*UMR CNRS 6613, Institut d'Acoustique - Graduate School (IA-GS),*

*CNRS, Le Mans Université, France.*

Charlie Bricault and Sébastien Goude

*Vibrations & Acoustics Laboratory, Valeo Thermal Systems, France.*

Ping Sheng

*Department of Physics, HKUST, Clear Water Bay, Kowloon, Hong Kong, China.*

## Abstract

In lossy acoustical systems, sum rules obtained from passivity are of primary importance for guiding the design of subwavelength passive treatments. When the target spectrum is provided in some finite frequency bands, these sum rules can be directly used for a priori estimates on the required treatment dimensions. The theory of Herglotz function is applied systematically to derive sum rules for unidimensional scattering problems relying on passive acoustic treatments which are generally made of rigid, motionless, and sub-wavelength structures saturated by air. Using the concepts of admittance/impedance passivity and scattering passivity, the surface admittance/impedance and the reflection/transmission coefficients are used to construct a number of general sum rules. Examples are provided showing how to use these sum rules to evaluate the minimum required dimensions for passive acoustic treatments without any specific design.


## I. INTRODUCTION

Passivity is an inherent property satisfied by many physical systems. In particular, for a continuous, causal, linear, and time-translational invariant system, passivity may lead to sum rules and impose fundamental constraints on the system.

Generally speaking, sum rules are integral identities of the form $\int_0^\infty \omega^{-n} A(\omega) \mathrm{d}\omega = C$, where $\omega$ refers to the angular frequency, $A(\omega) \geq 0$ is closely related to the frequency response function of the system, $n$ is an integer included in the weighting factor $\omega^{-n}$, and the constant $C \geq 0$ is determined by intrinsic properties of the system, which are related to static and dynamic limits of the system response. Because the integrand is non-negative, the integration within finite frequency range provides a lower bound of $C$, which indicates a fundamental constraint satisfied by the system.

In order to derive sum rules and fundamental constraints of a given system, the Kramers–Kronig relations [1, 2] and the Bode gain-phase relation (or modified Kramers–Kronig relation) [3–5] are commonly adopted. Practical examples can be found in network theory [6, 7], optics [8], electromagnetism [9], acoustics [10–12], nuclear physics [13], feedback control systems and filters [14], etc. Note however that additional assumptions are usually made on the systems [8, 15]. For instance, the response function is assumed to be a rational function in order to apply the Cauchy integral formula [15]. To consider more general cases with non-rational response functions for instance, one can build on the mathematical framework

developed by Bernland *et al.* [15]. This approach relies on the properties of Herglotz functions [8, 16] and has been used for various applications in electromagnetism, considering both lossless and lossy systems [17–21].

In contrast to electromagnetism, viscothermal losses usually play significant roles in the designs of passive treatments when we focus on acoustical systems in air, e.g., broadband absorbers [22–26], silencers [27, 28], meta-diffusers [29, 30], etc. See Refs. [31–35] and the references therein for other applications. Moreover, in lossy acoustical systems, the static/dynamic limits of the system response (and the aforementioned integral constant $C$) can be explicitly expressed by relevant spatial dimensions (i.e. total length or volume) as well as lumped structural parameters (i.e. porosity, tortuosity, etc.) of the system. Note that although these lumped parameters are unknowns without a specific design, their ranges and bounds are well known, e.g., $(0, 1]$ and $[1, \infty)$ for the porosity and the tortuosity, respectively [36]. Thus, this feature of lossy acoustical system allows a priori estimates on the required spatial dimensions for any given target spectrum, which is of primary importance for the design of subwavelength passive treatments: whenever some information of the relevant response function (i.e. the design target) is known or assumed within finite frequency bands, sum rules of the system can be directly used to evaluate the lower bound of the required treatment size.

For most of the commonly used acoustical treatments, the system response functions are not rational functions, such as the acoustic impedance of a quarter-wavelength resonator, which is a cotangent function of frequency, and the radiation impedance of a baffled circular piston or orifice, which is related to Bessel functions [37]. Thus, in this work we revisit the generalized theory based on the Herglotz functions [15] to derive and analyze the sum rules and fundamental constraints for lossy acoustical systems in unidimensional (1D) scattering problems. In Sec. II, the mathematical framework of the theory of Herglotz function is recalled from Ref. [15]. The transfer matrix modelling of the considered scattering problems is described in Sec. III.A. The sum rules and fundamental constraints are then derived and discussed for a rigid-boundary reflection problem (Sec. III.B), a soft-boundary reflection problem (Sec. III.C) and a transmission problem (Sec. III.D). In Sec. IV, two specific examples are given to explain how to evaluate the required minimum treatment size by using these sum rules. Conclusions are drawn in Sec. V. Validations and parametric studies of the derived sum rules are also provided in the Appendix.

## II. SUM RULES AND FUNDAMENTAL CONSTRAINTS FOR A PASSIVE UNI-DIMENSIONAL SYSTEM

For a continuous, causal, linear, and time-translational invariant system, the output of the system $Y(t)$ can be expressed as a convolution between the input $X(t)$ and the Green's function $G(t)$:

$$Y(t) = \int_0^\infty G(\tau)X(t-\tau)\mathrm{d}\tau, \tag{1}$$

where $\tau$ is the retarded time. Due to the causality of the system, $G(\tau) = 0$ for $\tau < 0$. After a time-domain Fourier transform, the convolution reduces to a product in the frequency domain which provides the definition of the frequency response function

$$\tilde{G}(\omega) = \frac{\tilde{Y}(\omega)}{\tilde{X}(\omega)}. \tag{2}$$

Note that in this work we use the following Fourier transformation pair

$$\tilde{f}(\omega) = \int_{-\infty}^{+\infty} f(t)\mathrm{e}^{\mathrm{i}\omega t}\mathrm{d}t, \tag{3a}$$

$$f(t) = \frac{1}{2\pi}\int_{-\infty}^{+\infty} \tilde{f}(\omega)\mathrm{e}^{-\mathrm{i}\omega t}\mathrm{d}\omega. \tag{3b}$$

With the response function well-defined, two equivalent definitions of the passivity of a system are generally considered, namely the admittance/impedance passivity and the scattering passivity [15, 21]. For 1D scattering problems, the passivity of the system ensures that the flux of acoustic energy into the surface remains non-negative. When the surface admittance $\eta(\omega)$, or the impedance $\zeta(\omega) = 1/\eta(\omega)$ is the relevant frequency response function, the sign of the resistive part of the response function is therefore fixed (either non-negative or non-positive) depending on the definitions of $\eta$ and $\zeta$. Based on the non-negative-resistive-part definition, the admittance/impedance passivity implies that

$$\mathrm{Re}[\eta(\omega)] \geq 0, \quad \text{and} \quad \mathrm{Re}[\zeta(\omega)] \geq 0. \tag{4}$$

When enforcing the scattering passivity of the system, the reflection and transmission coefficients, $R(\omega)$ and $T(\omega)$, should be such that $0 \leq |R(\omega)|^2 + |T(\omega)|^2 \leq 1$, i.e., $-\ln[|R(\omega)|^2 +$

$|T(\omega)|^2] \geq 0$, or separately, $0 \leq |R(\omega)| \leq 1$, and $0 \leq |T(\omega)| \leq 1$, so that scattering passivity results in

$$-\ln|R(\omega)| \geq 0, \quad \text{and} \quad -\ln|T(\omega)| \geq 0. \tag{5}$$

These relations state that the energy output of the system cannot exceed the input energy.

Herglotz functions are particularly useful to analyze the response of a passive system, since they are directly related to non-negative valued functions. By definition, a Herglotz function $H(\omega)$ is a holomorphic function in the upper half complex $\omega$ plane that also satisfies $\mathrm{Im}[H(\omega)] \geq 0$ for $\mathrm{Im}(\omega) > 0$ [15, 16]. Based on the different descriptions of passivity mentioned above, two types of Herglotz functions can be introduced for the 1D scattering problem. For the admittance/impedance passivity Eq. (4), we define

$$H_1(\omega) = \mathrm{i}\eta(\omega), \tag{6a}$$

$$H_1(\omega) = \mathrm{i}\zeta(\omega). \tag{6b}$$

Analogously, for the scattering passivity in Eq. (5), two Herglotz functions can be defined as follows,

$$H_2(\omega) = -\mathrm{i}\log[-R(\omega)B(\omega)], \tag{7a}$$

$$H_2(\omega) = -\mathrm{i}\log[T(\omega)B(\omega)], \tag{7b}$$

where $\log(\cdot)$ is the complex logarithm, in contrast to the natural logarithm $\ln(\cdot)$ which stands for real variables. $B(\omega)$ is a Blaschke product introduced to remove the zeros of $R(\omega)$ or $T(\omega)$ from the upper half complex $\omega$ plane [9–11, 15]. This product is defined as follows

$$B(\omega) = \prod_n \frac{1-\omega/\omega_n^*}{1-\omega/\omega_n}, \tag{8}$$

where $\omega_n$ is the $n$-th zero of $R(\omega)$ or $T(\omega)$ in Eqs. (7) with $\mathrm{Im}(\omega_n) > 0$ and the star denotes the complex conjugate. Note that $-B(\omega)$ can be used instead of $B(\omega)$ when the soft-boundary reflection problem is considered. Also note that we will use different Herglotz functions for each passivity condition, i.e. either the form (a) or (b) in Eqs. (6) and (7), depending on their static and dynamic limits.

When the input/output functions are real-valued in the time domain, the Herglotz functions introduced in Eqs. (6) and (7) are symmetric, i.e. $H(\omega) = -H^*(-\omega^*)$ is satisfied.

From the representation theorem [15], the asymptotic expansions of a symmetric Herglotz function in the static limit ($\omega\hat{\to}0$) and the dynamic limit ($\omega\hat{\to}\infty$) can be written as:

$$H(\omega) = \frac{a_{-1}}{\omega} + a_1\omega + ... + a_{2N_0-1}\omega^{2N_0-1} + o(\omega^{2N_0-1}), \quad \text{when } \omega\hat{\to}0\ , \tag{9a}$$

$$H(\omega) = b_1\omega + \frac{b_{-1}}{\omega} + ... + \frac{b_{1-2N_\infty}}{\omega^{2N_\infty-1}} + o\left(\frac{1}{\omega^{2N_\infty-1}}\right), \quad \text{when } \omega\hat{\to}\infty\ , \tag{9b}$$

where $a_n$, $b_n$ are real coefficients, and $N_0$, $N_\infty$ are non-negative integers. Moreover, the expansions should be stopped whenever a term that does not satisfy the forms of Eqs. (9) appears (e.g. $\log\omega$, $\sqrt{\omega}$, constant or any even-order term of $\omega$). Note that the notation $\hat{\to}$ denotes the limit in the Stoltz domain $\theta \leq \arg\,\omega \leq \pi - \theta$, for any $0 < \theta \leq \pi/2$, in the complex $\omega$ plane rather than on the real axis. As shown in Ref. [15], the coefficients $a_n$ and $b_n$ in Eqs. (9) can then be used to construct a series of integral identities or sum rules:

$$\lim_{\varepsilon\to0^+}\lim_{\delta\to0^+}\frac{2}{\pi}\int_\varepsilon^{\varepsilon^{-1}}\frac{\mathrm{Im}[H(\omega+\mathrm{i}\delta)]}{\omega^{2n}}\mathrm{d}\omega = a_{2n-1} - b_{2n-1}, \tag{10}$$

where $n = 1 - N_\infty, ..., N_0$. Note that, not every symmetric Herglotz function does admit a sum rule. A trivial example is that $H(\omega) = \mathrm{i}C$, where $C > 0$. It is easy to validate that $H(\omega)$ is a symmetric Herglotz function, however, the leading terms of its asymptotic expansions are $a_0$ and $b_0$ terms, with which the general formula Eq. (10) is not applicable.

In each case considered in this work, the $n = 1$ sum rule is allowed. We have thus:

$$\frac{2}{\pi}\int_0^\infty\frac{\mathrm{Im}[H(\omega)]}{\omega^2}\mathrm{d}\omega = a_1 - b_1, \tag{11}$$

in which the integral from zero to infinity is a shorthand notation for the limits in Eq. (10). In the following sections, we will show that the diverging term $b_1\omega$ in the dynamic limit does not exist in most cases, i.e., $b_1 = 0$, so that the $n = 1$ sum rule only involves the static limit of the system. The only exception is the sum rule for $T(\omega)$ in the transmission problem. In this case, $b_1$, which represents the group delay [38] induced by the material layer, does not vanish. Hence, this particular sum rule is influenced by both the static and dynamic limits of the system.

## III. FUNDAMENTAL CONSTRAINTS FOR UNIDIMENSIONAL SCATTERING PROBLEMS

### A. Transfer matrix modelling of the system

We consider several 1D scattering problems in which an incident plane wave is scattered by an effective material with thickness $L$ as illustrated in Fig. 1. We assume that this material consists of rigid, motionless and sub-wavelength elements, e.g. tubes, cavities, perforations, porous materials, etc. Notice that these elements are not restricted to be merely inside the waveguide. Side branch elements could also be accounted for in this effective layer through the homogenization theory [34, 35]. All the elements as well as the waveguide is saturated by air with density $\rho_0$ and adiabatic sound speed $c_0$. The losses within the system are induced by viscothermal boundary layers near the no-slip and isothermal boundaries.

We start from the case in which the effective material is mirror symmetric, so that the acoustic behavior of the material can be modelled as an equivalent fluid layer with frequency-dependent effective parameters [34–36]. This configuration is subsequently generalized to account for multilayer structures which are locally mirror symmetric (each sub-layer is mirror symmetric).

Under the above assumptions, the state vector at $x = L$ can be related to that at $x = 0$ through the transfer matrix $\mathbf{T}$ of the single-layer system [34, 35]:

$$\begin{bmatrix} P(L) \\ U(L) \end{bmatrix} = \mathbf{T} \begin{bmatrix} P(0) \\ U(0) \end{bmatrix} = \begin{bmatrix} t_{11} & t_{12} \\ t_{21} & t_{22} \end{bmatrix} \begin{bmatrix} P(0) \\ U(0) \end{bmatrix}, \tag{12}$$

where $P = p/K_0$, $U = u/c_0$ refer to the dimensionless forms of acoustic pressure and particle velocity: the acoustic pressure $p$ and particle velocity $u$ are normalized by the adiabatic bulk modulus $K_0 = \rho_0 c_0^2$ and the sound speed $c_0$ of air, respectively. The elements of the transfer matrix are

$$t_{11} = t_{22} = \cos(k_\mathrm{e} L), \tag{13a}$$

$$t_{12} = \mathrm{i}\frac{z_\mathrm{e}}{z_0}\sin(k_\mathrm{e} L), \tag{13b}$$

$$t_{21} = \mathrm{i}\frac{z_0}{z_\mathrm{e}}\sin(k_\mathrm{e} L), \tag{13c}$$

in which $z_0 = \rho_0 c_0$ refers to the characteristic impedance of air. The effective parameters of the material are frequency-dependent, including its density $\rho_\mathrm{e}$, sound speed $c_\mathrm{e}$, characteristic

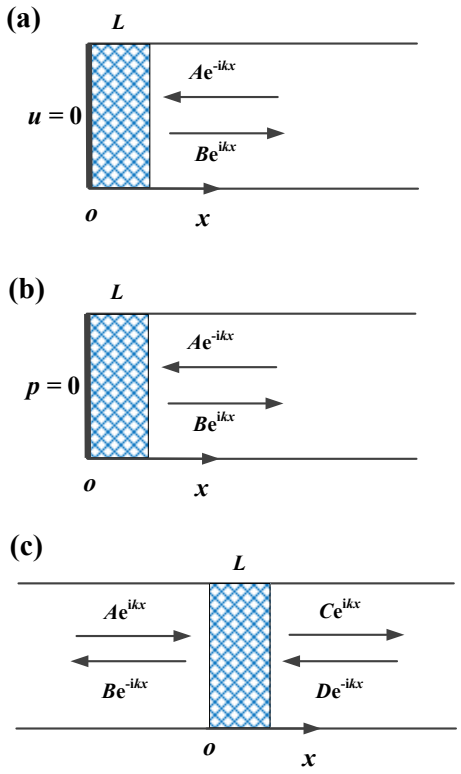


FIG. 1. The 1D scattering problem of a plane wave by a mirror-symmetric effective material: (a) Rigid-boundary reflection problem; (b) Soft-boundary reflection problem; (c) Transmission problem.

impedance $z_\mathrm{e} = \rho_\mathrm{e} c_\mathrm{e}$ and acoustic wavenumber $k_\mathrm{e} = \omega/c_\mathrm{e}$. The static and dynamic limits of these parameters can be rigorously evaluated; details are provided in Appendix A. Either for the 1D reflection problems or the 1D transmission problem, the acoustical response functions of the system can be expressed in terms of the elements of the transfer matrix.

### B. Rigid-boundary reflection problem

We first consider the reflection problem shown in Fig. 1(a) where a rigid boundary ($u = 0$) is imposed at one end of the material ($x = 0$). In this case, the relevant response functions are the surface admittance and the reflection coefficient at $x = L$. They are given by

$$\eta(\omega) = -\frac{t_{21}}{t_{11}} = -\mathrm{i}\frac{z_0}{z_\mathrm{e}}\tan(k_\mathrm{e}L), \tag{14a}$$

$$R(\omega) = \frac{t_{11} + t_{21}}{t_{11} - t_{21}} = \frac{z_\mathrm{e} + \mathrm{i}z_0\tan(k_\mathrm{e}L)}{z_\mathrm{e} - \mathrm{i}z_0\tan(k_\mathrm{e}L)}. \tag{14b}$$

With the choice of Herglotz functions $H_1$ and $H_2$ defined in Eq. (6a) and Eq. (7a), together with the Blaschke product $B$ from Eq. (8), the following $n = 1$ sum rules (as shown in Eq. (11)) can be derived for $\eta$ and $R$:

$$\frac{2c_0}{\pi}\frac{K_\mathrm{e}(0)}{K_0}\int_0^\infty \frac{1}{\omega^2}\mathrm{Re}[\eta(\omega)]\mathrm{d}\omega = L \ , \tag{15a}$$

$$\frac{c_0}{\pi}\frac{K_\mathrm{e}(0)}{K_0}\int_0^\infty \frac{-1}{\omega^2}\ln|R(\omega)|\,\mathrm{d}\omega \leq L \ . \tag{15b}$$

The first sum rule Eq. (15a) implies that when the thickness of a passive treatment is fixed, the resistance cannot be an arbitrarily chosen function of frequency. The second sum rule Eq. (15b) is an inequality because the static limit of the Blaschke product is dropped in the expansion of the Herglotz function (i.e. in the $a_1$ term), as explained in Appendix B. Besides, Eq. (15b) can be rearranged as a sum rule for the weighted absorption spectrum, due to the relation $\alpha(\omega) = 1 - |R(\omega)|^2$:

$$\frac{c_0}{2\pi}\frac{K_\mathrm{e}(0)}{K_0}\int_0^\infty \frac{-1}{\omega^2}\ln\left[1-\alpha(\omega)\right]\mathrm{d}\omega \leq L \ . \tag{16}$$

The sum rules (15a)–(16) are clearly controlled by the effective bulk modulus of the material $K_\mathrm{e} = \rho_\mathrm{e}c_\mathrm{e}^2$, which is expected since the low-frequency response of the system is monopolar (see Ref. [39–41] and Chap. 5 of Ref. [35]). The static limit of $K_\mathrm{e}$ can be easily derived (see p. 56 in Ref. [36]):

$$\frac{K_\mathrm{e}(0)}{K_0} = \frac{1}{\gamma\phi}, \tag{17}$$

where $\gamma = 1.4$ is the adiabatic index of air and $\phi$ is defined as the volume ratio between the saturating air and the whole layer. When all the elements of the material are fixed inside the waveguide, $\phi$ is the porosity of the material, and $\phi \leq 1$ is well satisfied. In the opposite, when side-branch elements are also included, $\phi$ could be larger than unity, because the volume of the the effective layer could be less than that of the material. The inequality (16) is in accordance with the results given in Refs. [11, 22], which provide a design criterion for the minimum total length of a broadband absorber. However, a difference exists in the evaluation of $K_\mathrm{e}(0)$. In Ref. [11], the system is modelled as a Lorentz oscillator, so that the losses are independent of frequency. As a result, the static limit of the effective bulk modulus tends to the adiabatic limit, which leads to $K_\mathrm{e}(0)/K_0 = 1/\phi$ (shown in the supplemental material of Ref. [11]). Conversely, the viscothermal losses in the system are considered here by introducing frequency-dependent effective parameters in the transfer matrix. As a

consequence, the effective bulk modulus tends to the isothermal limit, which leads to the additional factor $\gamma$ in Eq. (17).

From a practical point of view, the sum rule (16) can be used to provide guidelines for the design of acoustic treatments. For instance, if the aim is to achieve an absorption target $\alpha(\omega)$ then Eq. (16) provides a lower bound for the quantity $LK_0/K_\mathrm{e}(0)$. Since the porosity of the treatment can be estimated before a specific design, it is then possible to identify the minimum length $L_\mathrm{min}$ of the treatment to meet this absorption target. An example is provided in Sec. IV. Alternatively, for a given treatment with thickness $L$ and static limit $K_\mathrm{e}(0)$, Eq. (16) indicates the levels of the absorption spectrum that can be achieved with this treatment. Furthermore, the importance of the $1/\omega^2$ weighting terms in Eq. (16) should be emphasized. It implies that absorbing lower frequencies will require increasingly larger treatments. In other words, if the target absorption $\alpha$ is close to one at low frequencies, $L_\mathrm{min}$ will be particularly large.

The above sum rules are readily extended to the case of a multilayer composite material. In the static limit, the effective bulk modulus of the stratified medium can be obtained from those of the individual layers via a first-order homogenization scheme [34, 35]. This analysis directly results in the following sum rules:

$$\frac{2c_0}{\pi}\int_0^\infty \frac{1}{\omega^2}\mathrm{Re}[\eta(\omega)]\mathrm{d}\omega = \sum_i \left[\frac{K_0}{K_{\mathrm{e},i}(0)}L_i\right] \ , \tag{18a}$$

$$\frac{c_0}{\pi}\int_0^\infty \frac{-1}{\omega^2}\ln|R(\omega)|\,\mathrm{d}\omega \leq \sum_i \left[\frac{K_0}{K_{\mathrm{e},i}(0)}L_i\right] \ , \tag{18b}$$

$$\frac{c_0}{2\pi}\int_0^\infty \frac{-1}{\omega^2}\ln\left[1-\alpha(\omega)\right]\mathrm{d}\omega \leq \sum_i \left[\frac{K_0}{K_{\mathrm{e},i}(0)}L_i\right] \ , \tag{18c}$$

in which $K_{\mathrm{e},i}$, $L_i$ are the effective bulk modulus and length of the $i$-th layer, respectively.

### C. Soft-boundary reflection problem

We now consider the reflection problem depicted in Fig. 1(b) where a pressure-release boundary condition ($p = 0$) is used at $x = 0$. The relevant response functions are then

$$\begin{aligned} \zeta(\omega) &= -\frac{t_{12}}{t_{22}} = -\mathrm{i}\frac{z_\mathrm{e}}{z_0}\tan(k_\mathrm{e}L), \\ \text{or} \quad \eta(\omega) &= -\frac{t_{22}}{t_{12}} = \mathrm{i}\frac{z_0}{z_\mathrm{e}}\cot(k_\mathrm{e}L), \end{aligned} \tag{19a}$$

$$R(\omega) = \frac{t_{12} + t_{22}}{t_{12} - t_{22}} = \frac{z_\mathrm{e} - \mathrm{i}z_0 \cot(k_\mathrm{e} L)}{z_\mathrm{e} + \mathrm{i}z_0 \cot(k_\mathrm{e} L)}. \tag{19b}$$

In contrast to the rigid-boundary reflection problem, the static limits of $\zeta$, $\eta$, and $R$ depend on the normalized steady flow resistance of the layer (see Appendix B for the derivation), defined by

$$\xi = \frac{L\sigma}{z_0}, \tag{20}$$

in which $\sigma$ is the steady flow resistivity and $L\sigma$ measures the pressure loss caused by a low-speed steady flow across the layer. When in-series elements within the waveguide are considered, the steady flow resistivity can be expressed by $\sigma = (C_1\mu_0)/(r_H^2\phi)$. The positive real constant $C_1$ is determined by the geometry of the elements of the material. For example, for a circular tube $C_1 = 8$ while for a two-dimensional slit $C_1 = 3$ (see pp. 58–59 in Ref. [36]). The dynamic viscosity of air is denoted $\mu_0$ and $r_H = 2\bar{A}_\mathrm{c}/\bar{P}_\mathrm{c}$ is a typical length scale of the elements. $\bar{A}_\mathrm{c}$ and $\bar{P}_\mathrm{c}$ represent the averaged values of the area and perimeter of the cross sections of all the elements of the material, respectively. When all these have identical cross-sections, $r_H$ is one half of the hydraulic diameter (e.g. $r_H$ is the radius for a circular cross section) and is then the half-width of a two-dimensional slit.

The $n = 1$ sum rule in Eq. (11) is applicable only when the layer is either non-resistive ($\xi \to 0$) or highly resistive ($\xi \to \infty$). Apart from these two cases, the Herglotz functions $H_1$ and $H_2$ approaches to constants in the static and dynamic limits (i.e., $a_0$ and $b_0$ are the leading order terms in the asymptotic expansions as shown in Appendix B), and thus, no sum rule is available. However, it is still worth mentioning that, in the special case that the steady flow resistance of the layer matches the characteristic impedance of air (i.e. $\xi = 1$), the static limit of the reflection coefficient vanishes, i.e. $R(0) = 0$ (see the asymptotic expansion of $R(\omega)$ in Appendix B). In other words, the specific length $L = z_0/\sigma$ leads to perfect absorption in the static limit for any given material. This feature of soft-boundary reflection problem enables designs of space-saving absorbers in the ultra-low frequency range. In Ref. [42], a specific design has been proposed and validated experimentally.

In the next two subsections, we focus on the two distinct cases $\xi \to 0$ and $\xi \to \infty$ in which sum rules of the system are available. When the layer is non-resistive ($\xi \to 0$), the static limit $R(0) = -1$, and the response of the system is of dipolar nature [35, 39–41]. In the opposite, when the layer is highly resistive ($\xi \to \infty$), $R(0) = 1$ and a monopolar-type response is recovered.

*1. Non-resistive material: $\xi \to 0$*

First, we consider a non-resistive material. In contrast to the rigid-boundary reflection problem, the impedance $\zeta$ is used to construct the Herglotz function $H_1$ in Eq. (6b) because $\zeta(0) = O(\omega)$ in the static limit, which provides the $a_1$ term for the $n = 1$ sum rule, whereas $\eta(0)$ blows up. The Herglotz function $H_2$ is built from Eq. (7a) with the reflection coefficient $R$ and the Blaschke product $-B$ instead of $B$. These Herglotz functions $H_1$ and $H_2$ lead to the following sum rules:

$$\frac{2c_0}{\pi}\frac{\rho_0}{\mathrm{Re}[\rho_\mathrm{e}(0)]}\int_0^\infty \frac{1}{\omega^2}\mathrm{Re}[\zeta(\omega)]\mathrm{d}\omega = L \ , \tag{21a}$$

$$\frac{c_0}{\pi}\frac{\rho_0}{\mathrm{Re}[\rho_\mathrm{e}(0)]}\int_0^\infty \frac{-1}{\omega^2}\ln|R(\omega)|\,\mathrm{d}\omega \le L \ . \tag{21b}$$

Moreover, Eq. (21b) can be rearranged to obtain a sum rule for the absorption coefficient:

$$\frac{c_0}{2\pi}\frac{\rho_0}{\mathrm{Re}[\rho_\mathrm{e}(0)]}\int_0^\infty \frac{-1}{\omega^2}\ln\left[1-\alpha(\omega)\right]\mathrm{d}\omega \le L \ . \tag{22}$$

Due to the dipolar nature of the system, the real part of the effective density, $\mathrm{Re}(\rho_\mathrm{e})$, controls the above sum rules. Its static limit is given by

$$\frac{\mathrm{Re}[\rho_\mathrm{e}(0)]}{\rho_0} = \frac{C_2}{\phi}, \tag{23}$$

where the positive real constant $C_2$ depends on the cross-sectional geometry of the components of the material. When a material composed of in-series elements along the waveguide is considered, $C_2$ varies between 1.2 and 1.44 for commonly used shapes (see p. 64 in Ref. [36]).

The sum rules Eqs. (21) and (22) can be generalized to a multilayer material through the homogenization theory [34, 35], which yields

$$\frac{2c_0}{\pi}\int_0^\infty \frac{1}{\omega^2}\mathrm{Re}[\zeta(\omega)]\mathrm{d}\omega = \sum_i \left\{\frac{\mathrm{Re}[\rho_{\mathrm{e},i}(0)]}{\rho_0}L_i\right\} \ , \tag{24a}$$

$$\frac{c_0}{\pi}\int_0^\infty \frac{-1}{\omega^2}\ln|R(\omega)|\,\mathrm{d}\omega \le \sum_i \left\{\frac{\mathrm{Re}[\rho_{\mathrm{e},i}(0)]}{\rho_0}L_i\right\} \ , \tag{24b}$$

$$\frac{c_0}{2\pi}\int_0^\infty \frac{-1}{\omega^2}\ln\left[1-\alpha(\omega)\right]\mathrm{d}\omega \le \sum_i \left\{\frac{\mathrm{Re}[\rho_{\mathrm{e},i}(0)]}{\rho_0}L_i\right\} \ , \tag{24c}$$

where $\rho_{\mathrm{e},i}$ is the effective density of the $i$-th layer with length $L_i$.

*2. Highly resistive material: $\xi \to \infty$*

Second, a highly resistive material is considered. Similarly to the reflection problem with a rigid wall, the surface admittance $\eta$ and reflection coefficient $R$ are the relevant response functions. Correspondingly, the Herglotz functions $H_1$ and $H_2$ from Eq. (6a) and Eq. (7a) with Blaschke product $B$ in Eq. (8) are employed to yield the following $n = 1$ sum rules:

$$\frac{6c_0}{\pi}\frac{K_\mathrm{e}(0)}{K_0}\int_0^\infty \frac{1}{\omega^2}\mathrm{Re}[\eta(\omega)]\mathrm{d}\omega = L \ , \tag{25a}$$

$$\frac{3c_0}{\pi}\frac{K_\mathrm{e}(0)}{K_0}\int_0^\infty \frac{-1}{\omega^2}\ln|R(\omega)|\,\mathrm{d}\omega \leq L \ . \tag{25b}$$

The corresponding sum rule for the absorption coefficient is

$$\frac{3c_0}{2\pi}\frac{K_\mathrm{e}(0)}{K_0}\int_0^\infty \frac{-1}{\omega^2}\ln\left[1-\alpha(\omega)\right]\mathrm{d}\omega \leq L \ . \tag{26}$$

Note that the coefficients on the left-hand sides of Eqs. (25) and (26) are three times larger than those in the sum rules in Eqs. (15) and Eq. (16). This factor three arises from the first-order terms in $\omega$ in the low-frequency expansions of $\tan(k_\mathrm{e}L)/z_\mathrm{e}$ in the rigid-boundary reflection problem and of $\cot(k_\mathrm{e}L)/z_\mathrm{e}$ in the soft-boundary reflection problem, respectively (see Eqs. (14) and (19)). They are thus intrinsically related to the boundary condition, either rigid wall or pressure release boundary conditions.

For the multilayer case, the above sum rules can be generalized to

$$\frac{6c_0}{\pi}\int_0^\infty \frac{1}{\omega^2}\mathrm{Re}[\eta(\omega)]\mathrm{d}\omega = \sum_i \left[\frac{K_0}{K_{\mathrm{e},i}(0)}L_i\right] \ , \tag{27a}$$

$$\frac{3c_0}{\pi}\int_0^\infty \frac{-1}{\omega^2}\ln|R(\omega)|\,\mathrm{d}\omega \leq \sum_i \left[\frac{K_0}{K_{\mathrm{e},i}(0)}L_i\right] \ , \tag{27b}$$

$$\frac{3c_0}{2\pi}\int_0^\infty \frac{-1}{\omega^2}\ln\left[1-\alpha(\omega)\right]\mathrm{d}\omega \leq \sum_i \left[\frac{K_0}{K_{\mathrm{e},i}(0)}L_i\right] \ , \tag{27c}$$

where $K_{\mathrm{e},i}$ is the effective bulk modulus of the $i$-th layer with length $L_i$.

### D. Transmission problem

For a non-reciprocal and asymmetric system, the reflection and transmission coefficients in the transmission problem are given by

$$\begin{aligned} R^{-}(\omega) &= \frac{-t_{11}-t_{12}+t_{21}+t_{22}}{t_{11}-t_{12}-t_{21}+t_{22}} \\ &= \frac{\mathrm{i}\tan(k_{\mathrm{e}}L)\left(\dfrac{z_0}{z_{\mathrm{e}}}-\dfrac{z_{\mathrm{e}}}{z_0}\right)}{2-\mathrm{i}\tan(k_{\mathrm{e}}L)\left(\dfrac{z_0}{z_{\mathrm{e}}}+\dfrac{z_{\mathrm{e}}}{z_0}\right)}, \end{aligned} \tag{28a}$$

$$\begin{aligned} T^{-}(\omega) &= \frac{2\mathrm{e}^{-\mathrm{i}k_0L}(t_{11}t_{22}-t_{12}t_{21})}{t_{11}-t_{12}-t_{21}+t_{22}} \\ &= \frac{2\mathrm{e}^{-\mathrm{i}k_0L}}{2\cos(k_{\mathrm{e}}L)-\mathrm{i}\sin(k_{\mathrm{e}}L)\left(\dfrac{z_0}{z_{\mathrm{e}}}+\dfrac{z_{\mathrm{e}}}{z_0}\right)}, \end{aligned} \tag{28b}$$

$$\begin{aligned} R^{+}(\omega) &= \frac{t_{11}-t_{12}+t_{21}-t_{22}}{t_{11}-t_{12}-t_{21}+t_{22}} \\ &= \frac{\mathrm{i}\tan(k_{\mathrm{e}}L)\left(\dfrac{z_0}{z_{\mathrm{e}}}-\dfrac{z_{\mathrm{e}}}{z_0}\right)}{2-\mathrm{i}\tan(k_{\mathrm{e}}L)\left(\dfrac{z_0}{z_{\mathrm{e}}}+\dfrac{z_{\mathrm{e}}}{z_0}\right)}, \end{aligned} \tag{28c}$$

$$\begin{aligned} T^{+}(\omega) &= \frac{2\mathrm{e}^{-\mathrm{i}k_0L}}{t_{11}-t_{12}-t_{21}+t_{22}} \\ &= \frac{2\mathrm{e}^{-\mathrm{i}k_0L}}{2\cos(k_{\mathrm{e}}L)-\mathrm{i}\sin(k_{\mathrm{e}}L)\left(\dfrac{z_0}{z_{\mathrm{e}}}+\dfrac{z_{\mathrm{e}}}{z_0}\right)}, \end{aligned} \tag{28d}$$

in which the superscripts $^-$ and $^+$ refer to the surface $x = 0$ and $x = L$, respectively. In the case shown in Fig. 1(c), we consider a reciprocal system, $t_{11}t_{22} - t_{12}t_{21} = 1$ and thus $T^{-}(\omega) = T^{+}(\omega) \equiv T(\omega)$. Moreover, for a mirror symmetric single layer, $R^{-}(\omega) = R^{+}(\omega) \equiv R(\omega)$, i.e., $t_{11} = t_{22}$. Similarly to the soft-boundary reflection problem, the static limits of both $T(\omega)$ and $R(\omega)$ depend on the steady flow resistance $\xi$.

When the material is non-resistive ($\xi \to 0$), $T(0) = 1$ and $R(0) = 0$. As a result, the $n = 1$ sum rule in Eq. (11) is available only for Herglotz functions constructed from the transmission coefficient $T(\omega)$. In contrast, when the material is highly resistive ($\xi \to \infty$), $T(0) = 0$ and $R(0) = 1$. Consequently, the sum rules with the reflection coefficient $R(\omega)$ can

be derived from Eq. (11). Similarly to the soft-boundary reflection problem, in other cases when $\xi$ possesses the moderate values the Herglotz functions $H_1$ and $H_2$ do not lead to sum rules. However, in the special case where $\xi = 2$, $R(0) = T(0) = 1/2$, so that the absorption coefficient, defined by $\alpha = 1 - |R|^2 - |T|^2$, reaches its maximum value in the static limit, i.e. $\alpha = 1/2$. Note that, the maximum absorption coefficient of a point scatterer in the transmission problem is 1/2 at any frequency. Proofs are given in Refs. [39, 41].

*1. Non-resistive material:* $\xi \to 0$

We first consider the case of a non-resistive material, $\xi \to 0$. By an analogy with the surface admittance in the reflection problem, a bilinear transformation, which maps the unit disc to the closed upper half plane (see p. 131 in Ref. [43]), is used to construct the Herglotz function $H_1$ with the transmission coefficient:

$$H_1(\omega) = \mathrm{i}\frac{1 - T(\omega)}{1 + T(\omega)}. \tag{29}$$

The other Herglotz function, $H_2$, is derived from Eq. (7b), with the Blaschke product $B$ in Eq. (8). It follows that the corresponding sum rules are

$$\frac{8c_0}{\pi}\frac{\displaystyle\int_0^\infty \frac{1}{\omega^2}\mathrm{Re}\left[\frac{1 - T(\omega)}{1 + T(\omega)}\right]\mathrm{d}\omega}{\dfrac{K_0}{K_\mathrm{e}(0)} + \dfrac{\mathrm{Re}[\rho_\mathrm{e}(0)]}{\rho_0} - 2} = L\ , \tag{30a}$$

$$\frac{4c_0}{\pi}\frac{\displaystyle\int_0^\infty \frac{-1}{\omega^2}\ln|T(\omega)|\,\mathrm{d}\omega}{\dfrac{K_0}{K_\mathrm{e}(0)} + \dfrac{\mathrm{Re}[\rho_\mathrm{e}(0)]}{\rho_0} - 2\dfrac{c_0}{c_\infty}} \leq L\ . \tag{30b}$$

In the static limit, the layer of composite material reduces to a point scatterer and thus the transmission problem can be interpreted as a linear combination of a monopolar- and a dipolar-type reflection problems [35, 39–41, 44]. As a consequence, both the effective bulk modulus and the effective density are involved in Eqs. (30). Note that the dynamic behavior of the system contributes to the second sum rule in Eq. (30b). $c_\infty$ refers to the dynamic limit of the effective sound speed, and can be evaluated by

$$\frac{c_\infty}{c_0} = \frac{1}{\sqrt{\tau_\infty}}, \tag{31}$$

where $\tau_\infty \geq 1$ is the tortuosity of the material (see p. 67 of Ref. [36]). According to Eqs. (17) and (23),

$$\frac{K_0}{K_\mathrm{e}(0)} + \frac{\mathrm{Re}[\rho_\mathrm{e}(0)]}{\rho_0} = \gamma\phi + \frac{C_2}{\phi}. \tag{32}$$

For any $\phi \geq 0$, it can be found that $\gamma\phi + C_2/\phi \geq 2\sqrt{\gamma C_2}$. In Ref. [45] and p. 82 of Ref. [36], $C_2$ is alternatively denoted as the static tortuosity, $\tau_0$, of the material. Moreover, according to Ref. [46], $\tau_0 \geq \tau_\infty$. Therefore, $\gamma\phi + C_2/\phi \geq 2\sqrt{\gamma\tau_\infty} > 2\sqrt{\tau_\infty}$, and it follows that

$$\frac{K_0}{K_\mathrm{e}(0)} + \frac{\mathrm{Re}[\rho_\mathrm{e}(0)]}{\rho_0} > 2\frac{c_0}{c_\infty} > 2, \tag{33}$$

which ensures that the left-hand sides of Eqs. (30) are positive. When the tortuosity $\tau_\infty$ is hard to evaluate before a specific design, $\tau_\infty = 1$ could be used, which results in a lower bound of $L$ when applying the sum rule in Eq. (30b).

To obtain the constraints on the transmission loss and the absorption coefficient, the relations $\mathrm{TL}(\omega) = -20\log_{10}|T(\omega)|$, and $1 - \alpha(\omega) = |T(\omega)|^2 + |R(\omega)|^2 \geq |T(\omega)|^2$ can be combined with Eq. (30b) to write

$$\frac{c_0 \ln 10}{5\pi} \frac{\displaystyle\int_0^\infty \frac{\mathrm{TL}(\omega)}{\omega^2}\mathrm{d}\omega}{\dfrac{K_0}{K_\mathrm{e}(0)} + \dfrac{\mathrm{Re}[\rho_\mathrm{e}(0)]}{\rho_0} - 2\dfrac{c_0}{c_\infty}} \leq L\ , \tag{34a}$$

$$\frac{2c_0}{\pi} \frac{\displaystyle\int_0^\infty \frac{-1}{\omega^2}\ln\left[1-\alpha(\omega)\right]\mathrm{d}\omega}{\dfrac{K_0}{K_\mathrm{e}(0)} + \dfrac{\mathrm{Re}[\rho_\mathrm{e}(0)]}{\rho_0} - 2\dfrac{c_0}{c_\infty}} \leq L\ . \tag{34b}$$

We then consider a multilayer material. The reciprocity of the system still holds, so that $T^-(\omega) = T^+(\omega)$, but this system can then become asymmetric and consequently $R^-(\omega)$ and $R^+(\omega)$ might be different. In the low-frequency regime, the asymmetric part can be modelled by introducing the Willis coupling constant [47–49], when the homogenization method is applied. The coupling constant appears as a second-order term of $\omega$, and thus, the system falls back to a symmetric one in the static limit. However, the dynamic limit has to be derived from the transfer matrix of the entire system. These considerations provide a generalization of the sum rules in Eqs. (30) and (34):

$$\begin{aligned} &\frac{8c_0}{\pi}\int_0^\infty \frac{1}{\omega^2}\mathrm{Re}\left[\frac{1-T(\omega)}{1+T(\omega)}\right]\mathrm{d}\omega \\ &= \sum_i L_i \left\{\frac{K_0}{K_{\mathrm{e},i}(0)} + \frac{\mathrm{Re}[\rho_{\mathrm{e},i}(0)]}{\rho_0} - 2\right\}\ , \end{aligned} \tag{35a}$$

$$\frac{4c_0}{\pi}\int_0^\infty \frac{-1}{\omega^2}\ln|T(\omega)|\mathrm{d}\omega \leq \sum_i L_i\left\{\frac{K_0}{K_{\mathrm{e},i}(0)}+\frac{\mathrm{Re}[\rho_{\mathrm{e},i}(0)]}{\rho_0}-2\frac{c_0}{c_{\infty,i}}\right\}, \tag{35b}$$

$$\frac{c_0\ln 10}{5\pi}\int_0^\infty \frac{\mathrm{TL}(\omega)}{\omega^2}\mathrm{d}\omega \leq \sum_i L_i\left\{\frac{K_0}{K_{\mathrm{e},i}(0)}+\frac{\mathrm{Re}[\rho_{\mathrm{e},i}(0)]}{\rho_0}-2\frac{c_0}{c_{\infty,i}}\right\}, \tag{35c}$$

$$\frac{2c_0}{\pi}\int_0^\infty \frac{-1}{\omega^2}\ln\left[1-\alpha(\omega)\right]\mathrm{d}\omega \leq \sum_i L_i\left\{\frac{K_0}{K_{\mathrm{e},i}(0)}+\frac{\mathrm{Re}[\rho_{\mathrm{e},i}(0)]}{\rho_0}-2\frac{c_0}{c_{\infty,i}}\right\}, \tag{35d}$$

in which $K_{\mathrm{e},i}$, $\rho_{\mathrm{e},i}$ are the effective bulk modulus and density, respectively, $c_{\infty,i}$ denotes the dynamic limit of the effective sound speed of the $i$-th layer with length $L_i$.

*2. Highly resistive material: $\xi \to \infty$*

For the transmission problem with a highly resistive material, the relevant response functions are the surface admittance

$$\eta^{\pm}(\omega) = \frac{1-R^{\pm}(\omega)}{1+R^{\pm}(\omega)}, \tag{36}$$

and the reflection coefficients $R^{\pm}(\omega)$. Since the material is considered mirror symmetric, both $\eta$ and $R$ are identical on either side. It follows that the Herglotz functions $H_1$ and $H_2$ are defined in Eqs. (6a) and (7a) with the Blaschke product in Eq. (8).

It is found that, the sum rules in this situation take exactly the same form as in Eqs. (25) and Eq. (26) in the soft-boundary reflection problem. The details of the asymptotic expansions of $H_1$ and $H_2$ are available in Appendix B. A multilayer generalization directly results in sum rules expressed by Eqs. (27), considering that the multilayer material still has the mirror symmetry in the static limit because the Willis material falls back to be symmetric.

## IV. APPLICATIONS OF THE SUM RULES

The derived sum rules relate the target spectrum of the relevant response functions to the static/dynamic limits of the equivalent parameters as well as the total length of the layer

(or the length of each layer). Thus, the required minimum total length of the treatment can be predicted before any specific design provided these limits are well predicted by a priori estimates on the porosity and the tortuosity. Two specific examples are given in this section to show the practical applications of the sum rules.

The first example deals with the sum rule of a broadband absorber in the rigid-boundary reflection problem: when a target absorption spectrum is provided, the sum rule can be used to evaluate the required minimum length of the absorber. Apart from the rigid-boundary reflection problem, all the sum rules derived in the soft-boundary reflection problem and the transmission problem depend on the steady flow resistance $\xi = L\sigma/z_0$. Therefore, an estimation of $\xi$ should be made to select the suitable sum rule. After the prediction of the minimum length, the value of $\xi$ should be examined. However, some cases exist for which $\xi$ can be easily fixed. These cases are of great importance in practical applications as well. The second example of this section focuses on the transmission problem of a ring-shaped muffler in parallel of the circular waveguide with grazing incident wave. When the viscothermal losses in the main duct can be neglected compared with those induced by the muffler, this scenario provides a case for which the effective layer is perfectly non-resistive, i.e. $\xi = 0$. It is shown that, when a target transmission loss spectrum is provided, the required minimum volume of the muffler can be predicted by the sum rule.

It should be noticed that due to the weighting factor $1/\omega^2$ in all the derived sum rules, the low-frequency spectrum of the target response function has a dramatic effect on the predicted total length of the system. However, without a specific design, there is usually a lack of details on the target function near the static limit. In both of the following examples, we fix this problem by interpolating the target spectra, in which the basis functions are properly chosen to preserve the asymptotic behaviors of the corresponding target functions in the static limit.

### A. Minimum length of a broadband absorber for a target absorption spectrum in the rigid-boundary reflection problem

As illustrated in Fig. (1a), we assume that the layer of material is composed of in-series elements or laminates fixed within the waveguide. According to the sum rule Eq. (16), the

minimum length can be predicted by

$$L_{\min} = \frac{-c_0}{4\pi^2\gamma\phi}\int_{f_1}^{f_2}\frac{\ln\left[1-\alpha_{\mathrm{T}}(f)\right]}{f^2}\mathrm{d}f, \tag{37}$$

where $\alpha_{\mathrm{T}}$ is the target spectrum, given within the frequency range $[f_1,\ f_2]$. From Eq. (37), it is clear that the integral blows up if we choose $\alpha_{\mathrm{T}} = 1$ from $f_1$ to $f_2$. This implies that, in principle broadband-perfect absorption cannot be realized by an absorber with finite length. In fact, if perfect absorption is achieved in a finite frequency range, $\alpha = 1$ is guaranteed at any frequency. Provided that the reflection coefficient $R(\omega)$ is a constant zero within a finite interval, then $R(\omega)$ equals to the same constant in the whole complex $\omega$ plane, due to the Cauchy-Riemann conditions [43, 50] satisfied by real and imaginary parts of a holomorphic function. However, this does not prevent perfect absorption occurring at discrete frequencies. Moreover, when perfect absorption is achieved, $\alpha$ should be less than unity in the bands between these discrete frequencies [23].

In practical applications, the target spectrum is usually presented in octave bands or 1/3 octave bands. In contrast, a simplified target spectrum is employed here. We assume that the absorption coefficient is larger than 0.3, 0.6, and 0.9 at 100 Hz, 500 Hz, and 2500 Hz, respectively. According to Eq. (37), it seems that the most efficient absorber (which has the minimum length) is achieved when $\alpha_{\mathrm{T}}$ is exactly zero outside the considered frequency band. However, this idealized target spectrum is not physically accessible. Particularly, the absorption coefficient possesses the quadratic nature in the low frequency range [22], i.e. $\alpha \sim (k_0 L)^2$. Thus, in this case we assume $\alpha_{\mathrm{T}} = 30(f/10^3)^2$ when $f \leq 100$ Hz. For higher frequency range, the target spectrum $\alpha_{\mathrm{T}}$ is derived from interpolations:

$$\alpha_{\mathrm{T}}(f) = \begin{cases} 30\left(\dfrac{f}{10^3}\right)^2 & f \leq 100 \text{ Hz} \\ 0.75\left(\dfrac{f}{10^3}\right) + 0.225 & 100 \text{ Hz} \leq f \leq 500 \text{ Hz} \\ 0.15\left(\dfrac{f}{10^3}\right) + 0.525 & 500 \text{ Hz} \leq f \leq 2500 \text{ Hz} \\ 0.9 & f \geq 2500 \text{ Hz} \end{cases}. \tag{38}$$

With this target $\alpha_{\mathrm{T}}$, the minimum length is predicted from Eq. (37), which results in $L_{\min} = 6.1$ cm. The effect of the low-frequency spectrum of $\alpha_{\mathrm{T}}$ on $L_{\min}$ is further studied through calculation of Eq. (37) within the frequency band $[f, \infty)$. The results are illustrated

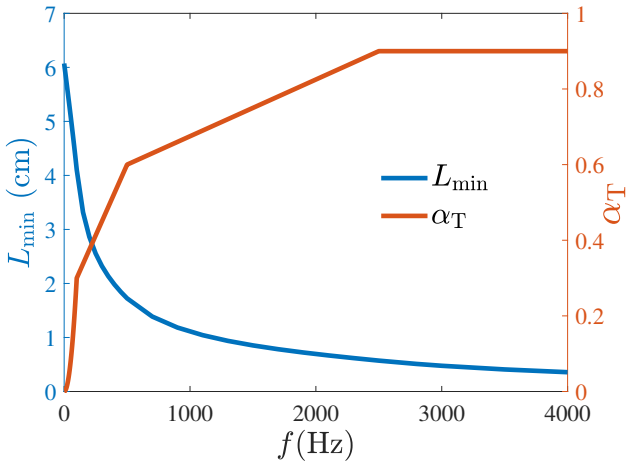


FIG. 2. Target absorption spectrum $\alpha_{\mathrm{T}}$ and the minimum length $L_{\min}$ evaluated from the contribution of $\alpha_{\mathrm{T}}$ within the frequency range $[f, \infty)$.

in Fig. (2). It is found that, although $\alpha_{\mathrm{T}}$ is less than 0.3 below 100 Hz, the low-frequency spectrum still has a significant effect on $L_{\min}$. When we start the sum-rule integration at $f = 100$ Hz, $L_{\min}$ reduces to 4.1 cm, which is 30% lower than that predicted by the full spectrum. In contrast, the high-frequency spectrum (although $\alpha_{\mathrm{T}}$ is close to one) has a much less effect on $L_{\min}$. If we set $\alpha_{\mathrm{T}} = 0$ for $f \geq 2500$ Hz, the predicted $L_{\min}$ is merely 10% less than 6.1 cm.

In the above calculations, the porosity $\phi = 1$ is used. For commonly used porous materials, $\phi$ is very close to unity as shown in Ref. [51]. For other in-series structures used within the waveguide, when $\phi$ is difficult to evaluate, $\phi = 1$ can be used as well to predict the lower bound of $L_{\min}$.

### B. Minimum volume of a ring-shaped muffler for a target transmission loss spectrum with grazing incident wave

We consider the transmission problem of a ring-shaped muffler with length $L$ in the axial direction and thickness $H$ in the radial direction, as illustrated in Fig. (3). This muffler is set in parallel of a circular waveguide whose radius is $R_{\mathrm{d}}$. It is modelled as an equivalent material, with a rigid outer boundary at $r = R_{\mathrm{d}} + H$. The muffler is assumed to be locally reacting so that there is only 1D radial wave within the equivalent material. Then,

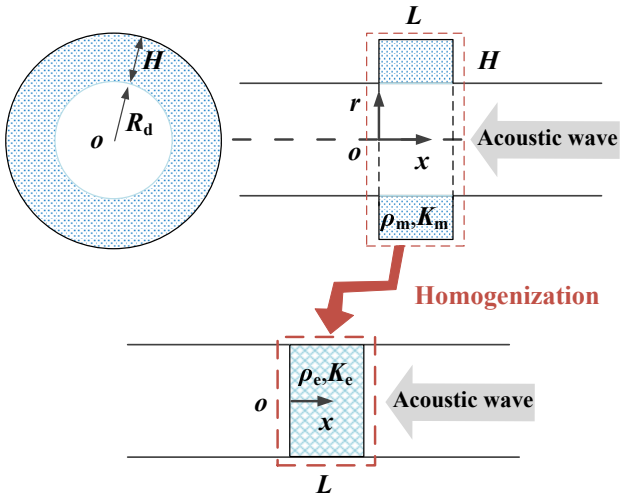


FIG. 3. Effective layer introduced by a ring-shaped muffler in parallel of a circular waveguide. The muffler is filled with a uniform material whose effective density and bulk modulus are $\rho_\mathrm{m}$ and $K_\mathrm{m}$ respectively. Via the homogenization method, the acoustic performance of the muffler can be well described by the layer with effective parameters $\rho_\mathrm{e}$ and $K_\mathrm{e}$.

the viscothermal losses within the material can be modelled by complex-valued effective parameters: the effective density and bulk modulus of the material are denoted by $\rho_\mathrm{m}$ and $K_\mathrm{m}$, respectively. In contrast, losses in the main waveguide are neglected.

Under these assumptions, the effect of the muffler on the wave propagation in the waveguide can be well described by introducing an effective layer with the same axial length $L$. Then, the static and dynamic limits of the effective parameters of the layer could be evaluated and the sum rules in the 1D transmission problem can be directly applied. Via the zeroth-order homogenization scheme [34, 35, 49], the static limit of the effective density of the layer ($\rho_\mathrm{e}(0)$) reduces to that of the medium within the waveguide, whereas the static limit of the effective bulk modulus ($K_\mathrm{e}(0)$) can be expressed by that of each component weighted by the volume. It follows that

$$\frac{\rho_\mathrm{e}(0)}{\rho_0} = 1, \tag{39a}$$

$$\frac{K_\mathrm{e}(0)}{K_0} = 1 + \frac{V}{V_\mathrm{e}}\frac{K_\mathrm{m}(0)}{K_0} = 1 + \frac{V}{V_\mathrm{e}}\frac{1}{\gamma\phi_\mathrm{m}}, \tag{39b}$$

where $V_\mathrm{e} = \pi R_\mathrm{d}^2 L$ is the volume of the effective layer, $V = \pi(2R_\mathrm{d}H + H^2)L$ is the volume of the ring-shaped material, and $\phi_\mathrm{m}$ is the porosity of the material. Another derivation of the acoustical response of the system via the transfer matrix method is provided in

Appendix D. Because the imaginary part of the effective density is proportional to the steady flow resistivity in the static limit, Eq. (39a) implies that the effective layer is perfectly non-resistive ($\xi = 0$). Therefore, the sum rule Eq. (34a) can be directly used to evaluate the minimum length of the effective layer with the target transmission loss spectrum $\mathrm{TL_T}$ given. Note that under a grazing incident wave, $c_\infty$ (or $\tau_\infty$) of the effective layer is usually difficult to evaluate. Here $c_\infty = c_0$ (i.e., $\tau_\infty = 1$) is used as an approximation. With $\rho_\mathrm{e}(0)$, $K_\mathrm{e}(0)$ and $c_\infty$ provided, the sum rule Eq. (34a) can be rewritten as

$$V_{\min} = \frac{c_0 R_\mathrm{d}^2 \ln 10}{10\pi\gamma\phi_\mathrm{m}} \int_{f_1}^{f_2} \frac{\mathrm{TL_T}(f)}{f^2} \mathrm{d}f, \tag{40}$$

where $V_{\min} = \min[\pi(2R_\mathrm{d}H + H^2)L]$ denotes the minimum volume of the ring-shaped muffler.

We assume that the target transmission loss $\mathrm{TL_T}$ is larger than 2 dB, 12 dB, 8 dB and 2 dB at 250 Hz, 500 Hz, 1000 Hz, and 2000 Hz, respectively. The radius of the circular waveguide $R_\mathrm{d}$ is assumed to be 5 cm. Similarly to the previous example, the $\mathrm{TL_T}$ spectrum under 250 Hz is important for the prediction of the minimum volume. Since $|T(\omega)|^2 = 1 - A\omega^2 + o(\omega^2)$ at low frequency, where $A$ is a positive coefficient, the transmission loss also possesses the quadratic dependence on frequency near the static limit. Thus, the target spectrum $\mathrm{TL_T}$ is expressed by the following function:

$$\mathrm{TL_T}(f) = \begin{cases} 32\left(\dfrac{f}{10^3}\right)^2 & f \le 250 \text{ Hz} \\ 40\left(\dfrac{f}{10^3}\right) - 8 & 250 \text{ Hz} \le f \le 500 \text{ Hz} \\ -8\left(\dfrac{f}{10^3}\right) + 16 & 500 \text{ Hz} \le f \le 1000 \text{ Hz} \\ -6\left(\dfrac{f}{10^3}\right) + 14 & 1000 \text{ Hz} \le f \le 2000 \text{ Hz} \\ 2 & f \ge 2000 \text{ Hz} \end{cases} . \tag{41}$$

With $\mathrm{TL_T}$ provided, the effect of the given spectrum on the prediction of $V_{\min}$ can be analyzed. Results of parametric studies are illustrated in Fig. (4), where $V_{\min}(f)$ is calculated by Eq. (40) within the frequency band $[f, \infty)$, and $\phi_\mathrm{m} = 1$. If $\mathrm{TL_T}$ is approximated by zero when $f \le 250$ Hz, the underestimation of $V_{\min}$ is nearly 25%. In the opposite, the high-frequency spectrum of $\mathrm{TL_T}$ (e.g. $f > 1000$ Hz) does not contribute much to $V_{\min}$, as one would expect.

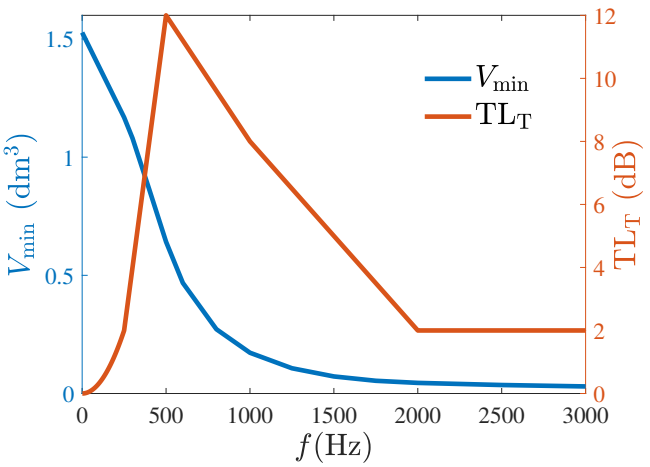


FIG. 4. Target transmission loss spectrum $\mathrm{TL_T}$ and the minimum volume $V_{\min}$ evaluated from the contribution of $\mathrm{TL_T}$ within the frequency range $[f, \infty)$.

## V. CONCLUSION

With the sum rules in lossy acoustical systems, the minimum size of a passive metamaterial is readily predicted from its target broadband response, which is of primary importance for guiding the design of subwavelength acoustical treatments.

In this work, the theory of Herglotz function is revisited and applied systematically to derive sum rules for 1D acoustical scattering problems, including the rigid/soft-boundary reflection and the transmission problems. The derivations in all the cases involve the following standard steps: a) Identify non-negative valued functions (i.e. Herglotz functions) from the relevant response functions, considering either admittance/impedance passivity or scattering passivity of the system. b) Analyze the asymptotic behaviors of these Herglotz functions in the static and dynamic limits. c) Derive the sum rules from the coefficients of the asymptotic expansions.

In the rigid-boundary reflection problem, the recently derived constraint for the absorption coefficient in Ref. [11] is recovered. Moreover, a new constraint for the surface admittance is obtained. In the soft-boundary reflection and the transmission problems, the asymptotic behaviors of Herglotz functions depend on the steady flow resistance of the effective material, i.e. $\xi = L\sigma/z_0$. Consequently, sum rules in these two problems exist merely when $\xi \to 0$ or $\xi \to \infty$, corresponding to cases in which the material is either non-resistive or highly resistive, respectively. Besides, in special cases where $\xi = 1$ or 2 in the soft-boundary

reflection or the transmission problem, the absorption coefficients can reach their maximum static-limit values, 1 or 1/2 respectively, although the considered Herglotz functions do not admit sum rules.

**ACKNOWLEDGMENTS**

Y. M., V. R.-G., G. G., J.-P. G., C. B. and S. G. gratefully acknowledge the support of Valeo. J.-P. G., V. R.-G. and P. S. would like to acknowledge the support of the ANR-RGC METARoom project (ANR-18-CE08-0021 and RGC A-HKUST601/18).

**Appendix A: Static/dynamic limits of the effective parameters**

It is assumed that the losses of the system arise from viscothermal effects near the no-slip and isothermal boundaries. Here, we fix the discussion on an in-series material inside the waveguide. When side-branch structures are included, the asymptotic expansions of the effective parameters of the material preserve the same dependence on $\omega$, but the coefficients should be interpreted differently.

For in-series material with porosity $\phi$, the asymptotic expansions can be directly evaluated [36]. In the static limit $\omega \hat{\to} 0$,

$$\frac{\rho_\mathrm{e}}{\rho_0} \hat{\to} \frac{1}{\phi}\left(\mathrm{i}\frac{C_1}{S_H^2} + C_2\right) + o(1) = \mathrm{i}\frac{\sigma}{\rho_0\omega} + \frac{C_2}{\phi} + o(1), \tag{A1a}$$

$$\frac{c_\mathrm{e}}{c_0} \hat{\to} (1-\mathrm{i})C_3 S_H + o(\sqrt{\omega}), \tag{A1b}$$

$$\frac{z_\mathrm{e}}{z_0} \hat{\to} \frac{(1+\mathrm{i})C_1 C_3}{\phi S_H} + o\left(\frac{1}{\sqrt{\omega}}\right), \tag{A1c}$$

$$\frac{K_\mathrm{e}}{K_0} \hat{\to} \frac{2C_1 C_3^2}{\phi} + o(1) = \frac{1}{\phi\gamma} + o(1), \tag{A1d}$$

where $C_1$, $C_2$ and $C_3$ are positive real constants (see pp. 55–57 of Ref. [36]),

$$S_H = r_H\sqrt{\frac{\omega}{\nu_0}} \tag{A2}$$

is the shear number of the cross section [52], $\nu_0 = \mu_0/\rho_0$ is the kinematic viscosity of air. Note that, from Eq. (A1a), the static limit of the density has a diverging imaginary part $\sim 1/\omega$. The real part tends to a constant and is written $C_2/\phi \equiv \mathrm{Re}[\rho_\mathrm{e}(0)]/\rho_0$. According

to Eq. (A1d), the static limit of the bulk modulus is real-valued and is written $2C_1C_3^2/\phi = 1/(\phi\gamma) \equiv K_{\mathrm{e}}(0)/K_0$.

Furthermore, in the dynamic limit $\omega\hat{\to}\infty$,

$$\frac{\rho_{\mathrm{e}}}{\rho_0}\hat{\to}\frac{\tau_\infty}{\phi}\left[1+(1+\mathrm{i})\frac{D_1}{S_H}\right]+o\left(\frac{1}{\sqrt{\omega}}\right), \tag{A3a}$$

$$\frac{c_{\mathrm{e}}}{c_0}\hat{\to}\frac{1}{\sqrt{\tau_\infty}}\left[1-(1+\mathrm{i})\frac{D_2}{S_H}\right]+o\left(\frac{1}{\sqrt{\omega}}\right), \tag{A3b}$$

$$\frac{z_{\mathrm{e}}}{z_0}\hat{\to}\frac{\sqrt{\tau_\infty}}{\phi}\left[1+\frac{(1+\mathrm{i})(D_1-D_2)}{S_H}\right]+o\left(\frac{1}{\sqrt{\omega}}\right), \tag{A3c}$$

$$\frac{K_{\mathrm{e}}}{K_0}\hat{\to}\frac{1}{\phi}\left[1+\frac{(1+\mathrm{i})(D_1-2D_2)}{S_H}\right]+o\left(\frac{1}{\sqrt{\omega}}\right), \tag{A3d}$$

where $D_1$, $D_2$ are positive real constants (see p. 71 of Ref. [36]), $\tau_\infty$ is the dynamic tortuosity. It is found that the dynamic limits of all these effective parameters are positive constants. Here, we denote $1/\sqrt{\tau_\infty} \equiv c_\infty/c_0$ and $\sqrt{\tau_\infty}/\phi \equiv z_\infty/z_0$.

## Appendix B: Asymptotic performances of the Herglotz functions

### 1. Rigid-boundary reflection problem

In the reflection problem with a rigid boundary, the relevant response functions are the surface admittance $\eta(\omega)$ and the reflection coefficient $R(\omega)$. Their asymptotic behaviors are given by

$$\eta(\omega)=\begin{cases}-\dfrac{\mathrm{i}\omega L}{c_0}\dfrac{K_0}{K_{\mathrm{e}}(0)}+o(\omega)\ ,\ \omega\hat{\to}0\\[2ex] \dfrac{z_0}{z_\infty}+o\left(1\right)\ ,\ \omega\hat{\to}\infty\end{cases}, \tag{B1}$$

and

$$R(\omega)=\begin{cases}1+\dfrac{2\mathrm{i}\omega L}{c_0}\dfrac{K_0}{K_{\mathrm{e}}(0)}+o(\omega)\ ,\ \omega\hat{\to}0\\[2ex] \dfrac{z_\infty-z_0}{z_\infty+z_0}+o\left(1\right)\ ,\ \omega\hat{\to}\infty\end{cases}. \tag{B2}$$

The following two Herglotz functions are introduced: $H_1(\omega) = \mathrm{i}\eta(\omega)$ and $H_2(\omega) = -\mathrm{i}\log[R(\omega)B(\omega)]$. Their asymptotic expansions are written as

$$H_1(\omega)=\begin{cases}\dfrac{\omega L}{c_0}\dfrac{K_0}{K_{\mathrm{e}}(0)}+o(\omega)\ ,\ \omega\hat{\to}0\\[2ex] O(1)\ ,\ \omega\hat{\to}\infty\end{cases}, \tag{B3}$$

and

$$H_2(\omega) = \begin{cases} \omega \left[ \dfrac{2L}{c_0} \dfrac{K_0}{K_\mathrm{e}(0)} + \displaystyle\sum_n \mathrm{Im}\left( \dfrac{1}{\omega_n} \right) \right] + o(\omega) \\ \leq \dfrac{2\omega L}{c_0} \dfrac{K_0}{K_\mathrm{e}(0)} + o(\omega) \ , \ \omega \hat{\to} 0 \\ O(1) \ , \ \omega \hat{\to} \infty \end{cases} . \tag{B4}$$

Note that the inequality in Eq. (B4) is derived with $\mathrm{Im}(\omega_n) > 0$.

From the above expansions, it is found that

$$a_1 = \frac{L}{c_0} \frac{K_0}{K_\mathrm{e}(0)}, \tag{B5a}$$

$$b_1 = 0, \tag{B5b}$$

for $H_1$, and

$$a_1 \leq \frac{2L}{c_0} \frac{K_0}{K_\mathrm{e}(0)}, \tag{B6a}$$

$$b_1 = 0, \tag{B6b}$$

for $H_2$.

### 2. Soft-boundary reflection problem

In the soft-boundary reflection problem, the relevant response functions include the impedance $\zeta(\omega)$, the admittance $\eta(\omega)$ and the reflection coefficient $R(\omega)$. The asymptotic behaviors of these functions are as follows

$$\zeta(\omega) = \begin{cases} \xi - \dfrac{\mathrm{i}\omega L}{c_0} \left\{ \dfrac{\mathrm{Re}[\rho_\mathrm{e}(0)]}{\rho_0} - \dfrac{\xi^2 K_0}{3K_\mathrm{e}(0)} \right\} + o(\omega), \\ \omega \hat{\to} 0 \\ \dfrac{z_\infty}{z_0} + o(1) \ , \ \omega \hat{\to} \infty \end{cases} , \tag{B7}$$

$$\eta(\omega) = \begin{cases} \dfrac{1}{\xi} - \dfrac{\mathrm{i}\omega L}{c_0} \left\{ \dfrac{K_0}{3K_\mathrm{e}(0)} - \dfrac{\mathrm{Re}[\rho_\mathrm{e}(0)]}{\xi^2 \rho_0} \right\} + o(\omega), \\ \omega \hat{\to} 0 \\ \dfrac{z_0}{z_\infty} + o(1) \ , \ \omega \hat{\to} \infty \end{cases} , \tag{B8}$$

$$R(\omega)=\begin{cases}\dfrac{\xi-1}{\xi+1}+\dfrac{2\mathrm{i}\omega L}{c_0}\dfrac{\dfrac{\xi^2}{3}-\dfrac{K_\mathrm{e}(0)}{K_0}\dfrac{\mathrm{Re}[\rho_\mathrm{e}(0)]}{\rho_0}}{(\xi+1)^2\dfrac{K_\mathrm{e}(0)}{K_0}}+o(\omega), \\ \omega\hat{\to}0 \\ \\ \dfrac{z_\infty-z_0}{z_\infty+z_0}+o\left(1\right)\ ,\ \omega\hat{\to}\infty\end{cases}, \tag{B9}$$

in which $\xi = C_1 L\nu_0/(\phi c_0 r_H^2) = L\sigma/z_0$.

*a. Non-resistive material:* $\xi \to 0$

When $\xi \to 0$, the Herglotz functions $H_1(\omega) = \mathrm{i}\zeta(\omega)$, and $H_2(\omega) = -\mathrm{i}\log[-R(\omega)B(\omega)]$ are considered. Their asymptotic expansions are

$$H_1(\omega)=\begin{cases}\dfrac{\omega L}{c_0}\dfrac{\mathrm{Re}[\rho_\mathrm{e}(0)]}{\rho_0}+o(\omega)\ ,\ \omega\hat{\to}0 \\ \\ O(1)\ ,\ \omega\hat{\to}\infty\end{cases}, \tag{B10}$$

and

$$H_2(\omega)=\begin{cases}\omega\left\{\dfrac{2L}{c_0}\dfrac{\mathrm{Re}[\rho_\mathrm{e}(0)]}{\rho_0}+\displaystyle\sum_n \mathrm{Im}\left(\frac{1}{\omega_n}\right)\right\}+o(\omega) \\ \leq \dfrac{2\omega L}{c_0}\dfrac{\mathrm{Re}[\rho_\mathrm{e}(0)]}{\rho_0}+o(\omega)\ ,\ \omega\hat{\to}0 \\ \\ O(1)\ ,\ \omega\hat{\to}\infty\end{cases}. \tag{B11}$$

It follows that, for $H_1$:

$$a_1 = \frac{L}{c_0}\frac{\mathrm{Re}[\rho_\mathrm{e}(0)]}{\rho_0}, \tag{B12a}$$

$$b_1 = 0, \tag{B12b}$$

and for $H_2$:

$$a_1 \leq \frac{2L}{c_0}\frac{\mathrm{Re}[\rho_\mathrm{e}(0)]}{\rho_0}, \tag{B13a}$$

$$b_1 = 0. \tag{B13b}$$

*b. Highly resistive material: $\xi \to \infty$*

When $\xi \to \infty$, the Herglotz functions $H_1(\omega) = \mathrm{i}\eta(\omega)$, and $H_2(\omega) = -\mathrm{i}\log[R(\omega)B(\omega)]$ are used. It follows that

$$H_1(\omega) = \begin{cases} \dfrac{\omega L}{3c_0}\dfrac{K_0}{K_\mathrm{e}(0)} + o(\omega)\ ,\ \omega\hat{\to}0 \\ \\ O(1)\ ,\ \omega\hat{\to}\infty \end{cases}, \tag{B14}$$

and

$$H_2(\omega) = \begin{cases} \omega\left[\dfrac{2L}{3c_0}\dfrac{K_0}{K_\mathrm{e}(0)} + \displaystyle\sum_n \mathrm{Im}\left(\frac{1}{\omega_n}\right)\right] + o(\omega) \\ \leq \dfrac{2\omega L}{3c_0}\dfrac{K_0}{K_\mathrm{e}(0)} + o(\omega)\ ,\ \omega\hat{\to}0 \\ \\ O(1)\ ,\ \omega\hat{\to}\infty \end{cases}. \tag{B15}$$

Therefore, for $H_1$:

$$a_1 = \frac{L}{3c_0}\frac{K_0}{K_\mathrm{e}(0)}, \tag{B16a}$$

$$b_1 = 0, \tag{B16b}$$

and for $H_2$:

$$a_1 \leq \frac{2L}{3c_0}\frac{K_0}{K_\mathrm{e}(0)}, \tag{B17a}$$

$$b_1 = 0. \tag{B17b}$$

### 3. Transmission problem

In the transmission problem, $R^-(\omega) = R^+(\omega) \equiv R(\omega)$, and $T^-(\omega) = T^+(\omega) \equiv T(\omega)$ when we consider a symmetric single-layer material. The asymptotic behaviors of $R(\omega)$ and $T(\omega)$ are provided by

$$R(\omega) = \begin{cases} \dfrac{\xi}{\xi+2} + \dfrac{2\mathrm{i}\omega L}{c_0}\dfrac{\dfrac{\xi^2}{3} + \xi + 1 - \dfrac{K_\mathrm{e}(0)}{K_0}\dfrac{\mathrm{Re}[\rho_\mathrm{e}(0)]}{\rho_0}}{(\xi+2)^2\dfrac{K_\mathrm{e}(0)}{K_0}} \\ +o(\omega)\ ,\ \omega\hat{\to}0 \\ \\ \dfrac{z_\infty - z_0}{z_\infty + z_0} + o(1)\ ,\ \omega\hat{\to}\infty \end{cases}, \tag{B18}$$

and

$$T(\omega)=\begin{cases}\dfrac{2}{\xi+2}+\dfrac{2\mathrm{i}\omega L}{c_0}\dfrac{1+\xi\left[\dfrac{\xi}{6}-\dfrac{K_\mathrm{e}(0)}{K_0}+1\right]+\dfrac{K_\mathrm{e}(0)}{K_0}\left\{\dfrac{\mathrm{Re}[\rho_\mathrm{e}(0)]}{\rho_0}-2\right\}}{(\xi+2)^2\dfrac{K_\mathrm{e}(0)}{K_0}}+o(\omega)\ ,\ \omega\hat{\to}0\\ o(1)\ ,\ \omega\hat{\to}\infty\end{cases}. \tag{B19}$$

*a. Non-resistive material:* $\xi\to 0$

Consider a non-resistive material with $\xi\to 0$. The Herglotz functions $H_1(\omega)=\mathrm{i}[1-T(\omega)]/[1+T(\omega)]$, and $H_2(\omega)=-\mathrm{i}\log[T(\omega)B(\omega)]$ are used. Then, the asymptotic expansions provide

$$H_1(\omega)=\begin{cases}\dfrac{\omega L}{4c_0}\left\{\dfrac{K_0}{K_\mathrm{e}(0)}+\dfrac{\mathrm{Re}[\rho_\mathrm{e}(0)]}{\rho_0}-2\right\}+o(\omega)\ ,\ \omega\hat{\to}0\\ O(1)\ ,\ \omega\hat{\to}\infty\end{cases}, \tag{B20}$$

and

$$H_2(\omega)=\begin{cases}\omega\left\{\dfrac{L}{2c_0}\left\{\dfrac{K_0}{K_\mathrm{e}(0)}+\dfrac{\mathrm{Re}[\rho_\mathrm{e}(0)]}{\rho_0}-2\right\}+\displaystyle\sum_n\mathrm{Im}\left(\frac{1}{\omega_n}\right)\right\}+o(\omega)\\ \le\omega\left\{\dfrac{L}{2c_0}\left\{\dfrac{K_0}{K_\mathrm{e}(0)}+\dfrac{\mathrm{Re}[\rho_\mathrm{e}(0)]}{\rho_0}-2\right\}\right\}+o(\omega)\ ,\ \omega\hat{\to}0\\ \dfrac{\omega L}{c_0}\left(\dfrac{c_\infty}{c_0}-1\right)+o(\omega)\ ,\ \omega\hat{\to}\infty\end{cases}. \tag{B21}$$

It can be found that, for $H_1$:

$$a_1=\frac{L}{4c_0}\left\{\frac{K_0}{K_\mathrm{e}(0)}+\frac{\mathrm{Re}[\rho_\mathrm{e}(0)]}{\rho_0}-2\right\}, \tag{B22a}$$

$$b_1=0, \tag{B22b}$$

and for $H_2$:

$$a_1\le\frac{L}{2c_0}\left\{\frac{K_0}{K_\mathrm{e}(0)}+\frac{\mathrm{Re}[\rho_\mathrm{e}(0)]}{\rho_0}-2\right\}, \tag{B23a}$$

$$b_1=\frac{L}{c_0}\left(\frac{c_\infty}{c_0}-1\right). \tag{B23b}$$

*b. Highly resistive material: $\xi \to \infty$*

When the material is highly resistive ($\xi \to \infty$), Herglotz functions $H_1(\omega) = \mathrm{i}\eta(\omega) = \mathrm{i}[1-R(\omega)]/[1+R(\omega)]$, and $H_2(\omega) = -\mathrm{i}\log[R(\omega)B(\omega)]$ are used. Their asymptotic expansions are

$$H_1(\omega) = \begin{cases} \dfrac{\omega L}{3c_0}\dfrac{K_0}{K_\mathrm{e}(0)} + o(\omega) \ , \ \omega \hat{\to} 0 \\ \\ O(1) \ , \ \omega \hat{\to} \infty \end{cases} , \tag{B24}$$

and

$$H_2(\omega) = \begin{cases} \omega\left[\dfrac{2L}{3c_0}\dfrac{K_0}{K_\mathrm{e}(0)} + \displaystyle\sum_n \mathrm{Im}\left(\frac{1}{\omega_n}\right)\right] + o(\omega) \\ \leq \dfrac{2\omega L}{3c_0}\dfrac{K_0}{K_\mathrm{e}(0)} + o(\omega) \ , \ \omega \hat{\to} 0 \\ \\ O(1) \ , \ \omega \hat{\to} \infty \end{cases} . \tag{B25}$$

For $H_1$:

$$a_1 = \frac{L}{3c_0}\frac{K_0}{K_\mathrm{e}(0)}, \tag{B26a}$$

$$b_1 = 0, \tag{B26b}$$

and for $H_2$:

$$a_1 \leq \frac{2L}{3c_0}\frac{K_0}{K_\mathrm{e}(0)} + o(\omega), \tag{B27a}$$

$$b_1 = 0. \tag{B27b}$$

The asymptotic behaviors of $H_1$ and $H_2$ are exactly those in the soft-boundary reflection problem with $\xi \to \infty$.

## Appendix C: Validations and parametric studies of the sum rules

TABLE I. Structural parameters of soft polyurethane foam (SPF) and glass wool.

| | $\phi$ | $\tau_\infty$ | $\Lambda$ ($\mu$m) | $\Lambda'$ ($\mu$m) | $q_0$ ($10^{-9}\mathrm{m}^2$) | $q_0'$ ($10^{-9}\mathrm{m}^2$) |
|---|---|---|---|---|---|---|
| SPF | 1.00 | 1.04 | 273 | 550 | 8.94 | 14.30 |
| glass wool | 0.96 | 1.00 | 37 | 100 | 0.39 | 0.58 |

In this Appendix, two types of air-saturated porous materials are employed to study and validate all the derived sum rules for a single-layer material. Specifically, soft polyurethane foam (SPF) and glass wool are considered, which have low and high steady flow resistivity respectively and can be used to construct a non-resistive and a highly resistive layer. The structural parameters of these materials are listed in Table. I, which are from the experimental studies in Ref. [51].

We follow the same steps in all the validations: (a) choose a specific material with a given length so that $\xi = L\sigma/z_0$ is either close to zero or much larger than unity; (b) calculate the considered response function; (c) predict the total length from the sum rule; (d) compare the predicted length and the given length.

In particular, sum rules of the first type (derived from admittance/impedance passivity) are equations rather than inequalities. Thus, the predicted lengths should be exactly the given lengths in these cases. Otherwise, the predicted lengths should be less than the given lengths when the lengths are predicted from sum rules of the second type or from either type but with finite frequency interval (in the following computations we consider both the full frequency range from 0 Hz to infinity and the audible range from 20 Hz to 20 kHz).

### 1. Causal models of effective parameters of air-saturated porous media

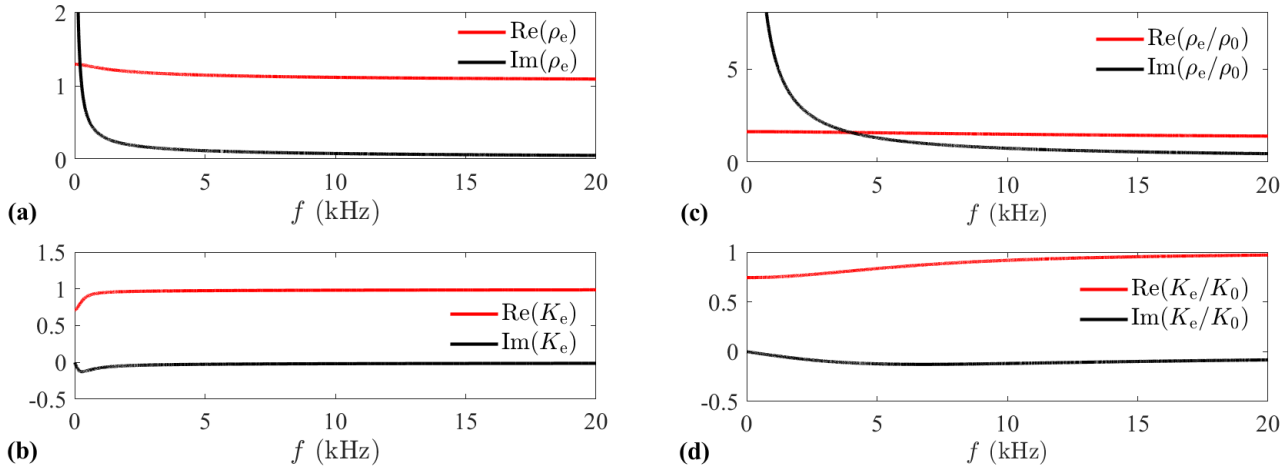


FIG. 5. Effective parameters of the two materials. SPF: (a) effective density; (b) effective bulk modulus. Glass wool: (c) effective density; (d) effective bulk modulus.

To predict the effective parameters of an air-saturated porous medium, we use the models from Refs. [53–55]

$$\frac{\rho_{\mathrm{e}}(\omega)}{\rho_0} = \frac{\tau_\infty}{\phi} - \frac{\nu_0}{\mathrm{i}\omega q_0}\sqrt{1 - \frac{\mathrm{i}\omega}{\nu_0}\left(\frac{2\tau_\infty q_0}{\phi\Lambda}\right)^2}, \tag{C1a}$$

$$\frac{K_{\mathrm{e}}(\omega)}{K_0} = \frac{1/\phi}{\gamma - \dfrac{\gamma - 1}{1 - \dfrac{\nu_0\phi}{\mathrm{i}\omega q_0'\mathrm{Pr}}\sqrt{1 - \dfrac{\mathrm{i}\omega\mathrm{Pr}}{\nu_0}\left(\dfrac{2q_0'}{\phi\Lambda'}\right)^2}}}, \tag{C1b}$$

where $q_0 = \mu_0/\sigma$ is the static viscous permeability, $q_0'$ is the static thermal permeability, Pr is the Prandtl number, $\Lambda$ and $\Lambda'$ are the characteristic viscous and thermal lengths respectively. In contrast to empirical formulas which mainly work in the moderate frequency range (e.g. Ref. [56]), the above models predict the right asymptotic behaviors in the static/dynamic limits, and moreover, satisfy causality (see also Ref. [57] and Chap. 5 of Ref. [36]. Therefore, Eqs. (C1) are used to validate the sum rules derived in this work. The effective parameters of SPF and wool are then calculated by Eqs. (C1). Results are shown in Fig. (5).

### 2. Validations of sum rules for a non-resistive material

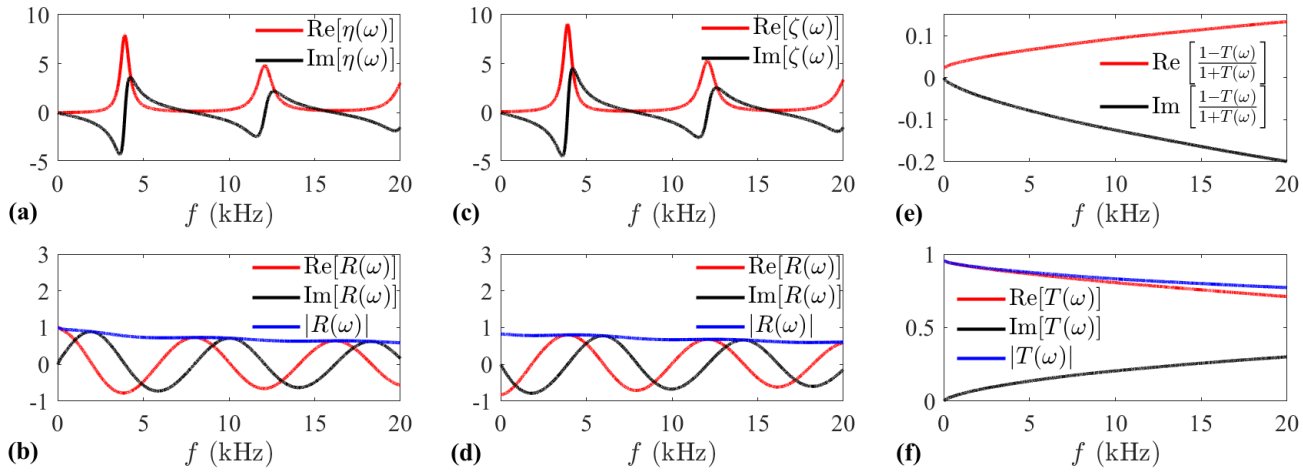


FIG. 6. Acoustical response of the SPF layer. In the rigid-boundary reflection problem: (a) specific acoustic admittance; (b) reflection coefficient. In the soft-boundary reflection problem: (c) specific acoustic impedance; (d) reflection coefficient. In the transmission problem: (e) response function built from the transmission coefficient; (f) transmission coefficient.

TABLE II. The total/minimum lengths of the SPF layer (whose length is 2 cm) predicted by sum rules.

| | Sum rules | $L_{\min}$ ($20 \sim 20$k Hz) | $L$ or $L_{\min}$ ($0 \sim \infty$ Hz) |
|---|---|---|---|
| Rigid-boundary reflection problem | $H_1$: Eq. (15a) | 1.8 cm | 2.0 cm |
| | $H_2$: Eq. (15b) | 0.6 cm | 0.7 cm |
| Soft-boundary reflection problem | $H_1$: Eq. (21a) | 1.9 cm | 2.0 cm |
| | $H_2$: Eq. (21b) | 0.2 cm | 0.2 cm |
| Transmission problem | $H_1$: Eq. (30a) | 1.6 cm | 2.0 cm |
| | $H_2$: Eq. (30b) | 1.7 cm | 2.0 cm |

To validate the sum rules for a non-resistive material, we consider a 2 cm layer of SPF. In this case, $\xi = 0.096 \ll 1$. The relevant response functions in reflection and transmission problems are derived and shown in Fig. (6). For the rigid-boundary reflection problem, the sum rules given by Eqs. (15) can be readily validated. However, in the soft-boundary reflection problem, sum rules expressed by Eqs. (21) hold merely in the limit $\xi \to 0$. Considering $\xi$ as a finite small quantity, the following modified forms of Herglotz functions are used in the computations to ensure the convergence of the integration:

$$H_1(\omega) = \mathrm{i}\left[\zeta(\omega) - \zeta(0)\right], \tag{C2a}$$

$$H_2(\omega) = -\mathrm{i}\log\left[\frac{R(\omega)B(\omega)}{R(0)}\right], \tag{C2b}$$

where the static limits are expressed as $\zeta(0) = \xi$ and $R(0) = (\xi - 1)/(\xi + 1)$. Similarly, in the transmission problem, the Herglotz functions used in the sum rules (Eqs. (30)) are rewritten as

$$H_1(\omega) = \mathrm{i}\left[\frac{1 - T(\omega)}{1 + T(\omega)} - \frac{1 - T(0)}{1 + T(0)}\right], \tag{C3a}$$

$$H_2(\omega) = -\mathrm{i}\log\left[\frac{T(\omega)B(\omega)}{T(0)}\right], \tag{C3b}$$

where $T(0) = 2/(2 + \xi)$. The prediction results on the total length or minimum length of the layer using different sum rules are collected in Table II.

### 3. Validations of sum rules for a highly resistive material

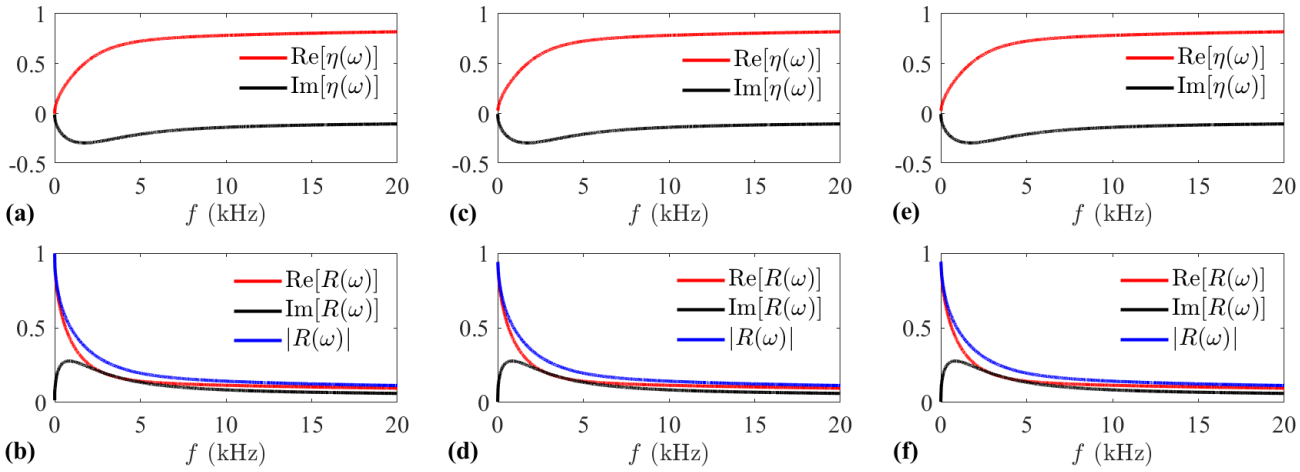


FIG. 7. Acoustical response of the glass wool layer. In the rigid-boundary reflection problem: (a) specific acoustic admittance; (b) reflection coefficient. In the soft-boundary reflection problem: (c) specific acoustic admittance; (d) reflection coefficient. In the transmission problem: (e) specific acoustic admittance; (f) reflection coefficient.

To validate the sum rules for a highly resistive material, a thick layer of glass wool (0.3 m) is considered. In this case, $\xi = 33.19 \gg 1$. The considered response functions in all the cases are shown in Fig. (7). The sum rules given by Eqs. (15) in the rigid-boundary reflection problem can be readily validated. Whereas in the soft-boundary reflection problem and the transmission problem, modified forms of Herglotz functions should be employed in the sum rules (in both case the sum rules are given by Eqs. (25)):

$$H_1(\omega) = \mathrm{i}\left[\eta(\omega) - \eta(0)\right], \tag{C4a}$$

$$H_2(\omega) = -\mathrm{i}\log\left[\frac{R(\omega)B(\omega)}{R(0)}\right], \tag{C4b}$$

where $\eta(0) = 1/\xi$, $R(0) = (\xi - 1)/(\xi + 1)$ for the soft-boundary reflection problem, and $\eta(0) = 1/(1 + \xi)$, $R(0) = \xi/(\xi + 2)$ for the transmission problem. Validation results are provided in Table III.

TABLE III. The total/minimum lengths of the glass wool layer (whose length is 0.3 m) predicted by sum rules.

| | Sum rules | $L_{\min}$ ($20 \sim 20$k Hz) | $L$ or $L_{\min}$ ($0 \sim \infty$ Hz) |
|---|---|---|---|
| Rigid-boundary reflection problem | $H_1$: Eq. (15a) | 0.12 m | 0.30 m |
| | $H_2$: Eq. (15b) | 0.12 m | 0.30 m |
| Soft-boundary reflection problem | $H_1$: Eq. (25a) | 0.24 m | 0.30 m |
| | $H_2$: Eq. (25b) | 0.24 m | 0.30 m |
| Transmission problem | $H_1$: Eq. (25a) | 0.24 m | 0.30 m |
| | $H_2$: Eq. (25b) | 0.24 m | 0.30 m |

### Appendix D: Transfer matrix modelling of the ring-shaped muffler

When the total length ($L$) of a ring-shaped muffler is much less than the considered wavelength, the effect of the material can be modelled by a point surface impedance $\zeta_{\mathrm{m}}$, which is located at $x = L/2$. Suppose that the muffler is locally reacting so that only 1D radial waves exist inside the material. Then, the surface impedance is expressed by

$$\begin{aligned} \zeta_{\mathrm{m}} &\equiv \left(\frac{p}{z_0 u}\right)_{r=R_{\mathrm{d}}} \\ &= \mathrm{i}\frac{z_{\mathrm{m}}}{z_0}\frac{J_1(k_{\mathrm{m}}r_2)N_0(k_{\mathrm{m}}r_1) - J_0(k_{\mathrm{m}}r_1)N_1(k_{\mathrm{m}}r_2)}{J_1(k_{\mathrm{m}}r_1)N_1(k_{\mathrm{m}}r_2) - J_1(k_{\mathrm{m}}r_2)N_1(k_{\mathrm{m}}r_1)}, \end{aligned} \tag{D1}$$

where $r_1 = R_{\mathrm{d}}$ and $r_2 = H + R_{\mathrm{d}}$ are the inner and outer radii, $z_{\mathrm{m}} = \rho_{\mathrm{m}} c_{\mathrm{m}}$ and $k_{\mathrm{m}} = \omega/c_{\mathrm{m}}$ are the effective impedance and wavenumber of the material, $J_{0,1}$ and $N_{0,1}$ are Bessel functions of first and second kinds, respectively. The transfer matrix of the system is

$$\begin{bmatrix} P(L) \\ U(L) \end{bmatrix} = \mathbf{T}_1\mathbf{T}_2\mathbf{T}_3 \begin{bmatrix} P(0) \\ U(0) \end{bmatrix} \equiv \mathbf{T} \begin{bmatrix} P(0) \\ U(0) \end{bmatrix}, \tag{D2}$$

where

$$\mathbf{T}_1 = \mathbf{T}_3 = \begin{bmatrix} \cos(k_0 L/2) & \mathrm{i}\sin(k_0 L/2) \\ \mathrm{i}\sin(k_0 L/2) & \cos(k_0 L/2) \end{bmatrix}, \tag{D3}$$

where the viscothermal losses inside the waveguide have been neglected, and

$$\mathbf{T}_2 = \begin{bmatrix} 1 & 0 \\ -\dfrac{2L}{R_\mathrm{d}}\dfrac{1}{\zeta_\mathrm{m}} & 1 \end{bmatrix}. \tag{D4}$$


[1] R. d. L. Kronig, On the theory of dispersion of x-rays, Journal of the Optical Society of America **12**, 547 (1926).

[2] H. A. Kramers, La diffusion de la lumiere par les atomes, in *Atti Cong. Intern. Fisica (Transactions of Volta Centenary Congress) Como*, Vol. 2 (1927) pp. 545–557.

[3] H. W. Bode, Relations between attenuation and phase in feedback amplifier design, The Bell System Technical Journal **19**, 421 (1940).

[4] K. E. Peiponen and J. J. Saarinen, Generalized Kramers–Kronig relations in nonlinear optical- and THz-spectroscopy, Reports on Progress in Physics **72**, 056401 (2009).

[5] J. Bechhoefer, Kramers–Kronig, Bode, and the meaning of zero, American Journal of Physics **79**, 1053 (2011).

[6] H. W. Bode, *Network analysis and feedback amplifier design* (van Nostrand, 1945).

[7] R. M. Fano, Theoretical limitations on the broadband matching of arbitrary impedances, Journal of the Franklin Institute **249**, 57 (1950).

[8] F. W. King, *Hilbert Transforms*, Vol. 2 (Cambridge University Press, 2009).

[9] K. N. Rozanov, Ultimate thickness to bandwidth ratio of radar absorbers, IEEE Transactions on Antennas and Propagation **48**, 1230 (2000).

[10] O. Acher, J. M. L. Bernard, P. Maréchal, A. Bardaine, and F. Levassort, Fundamental constraints on the performance of broadband ultrasonic matching structures and absorbers, The Journal of the Acoustical Society of America **125**, 1995 (2009).

[11] M. Yang, S. Chen, C. Fu, and P. Sheng, Optimal sound-absorbing structures, Materials Horizons **4**, 673 (2017).

[12] T. Bravo and C. Maury, Causally-guided acoustic optimization of single-layer rigidly-backed micro-perforated partitions: Theory, Journal of Sound and Vibration **520**, 116634 (2022).

[13] V. Pascalutsa, *Causality Rules: A light treatise on dispersion relations and sum rules*, IOP Concise Physics (Morgan & Claypool Publishers, 2018).

[14] M. M. Seron, J. H. Braslavsky, and G. C. Goodwin, *Fundamental limitations in filtering and control* (Springer Science & Business Media, 2012).

[15] A. Bernland, A. Luger, and M. Gustafsson, Sum rules and constraints on passive systems, Journal of Physics A: Mathematical and Theoretical **44**, 145205 (2011).

[16] H. M. Nussenzveig, *Causality and dispersion relations* (Academic Press, 1972).

[17] A. Bernland, *Integral Identities for Passive Systems and Spherical Waves in Scattering and Antenna Problems*, Ph.D. thesis, Department of Electrical and Information Technology, Lund University (2012).

[18] M. Gustafsson, An overview of sum rules and physical limitations for passive metamaterial structures, in *META13, the 4th International Conference on Metamaterials, Photonic Crystals and Plasmonics* (2013).

[19] M. Cassier and G. W. Milton, Bounds on Herglotz functions and fundamental limits of broadband passive quasistatic cloaking, Journal of Mathematical Physics **58**, 071504 (2017).

[20] M. Nedic, C. Ehrenborg, Y. Ivanenko, A. Ludvig-Osipov, S. Nordebo, A. Luger, L. Jonsson, D. Sjöberg, and M. Gustafsson, Herglotz functions and applications in electromagnetics (Institution of Engineering and Technology, 2020) pp. 491–514.

[21] A. Srivastava, Causality and passivity: From electromagnetism and network theory to metamaterials, Mechanics of Materials **154**, 103710 (2021).

[22] M. Yang and P. Sheng, Sound absorption structures: From porous media to acoustic metamaterials, Annual Review of Materials Research **47**, 83 (2017).

[23] N. Jiménez, V. Romero-García, V. Pagneux, and J.-P. Groby, Rainbow-trapping absorbers: Broadband, perfect and asymmetric sound absorption by subwavelength panels for transmission problems, Scientific Reports **7**, 1 (2017).

[24] V. Romero-García, N. Jiménez, G. Theocharis, V. Achilleos, A. Merkel, O. Richoux, V. Tournat, J.-P. Groby, and V. Pagneux, Design of acoustic metamaterials made of Helmholtz resonators for perfect absorption by using the complex frequency plane, Comptes Rendus. Physique **21**, 713 (2020).

[25] S. Huang, Z. Zhou, D. Li, T. Liu, X. Wang, J. Zhu, and Y. Li, Compact broadband acoustic sink with coherently coupled weak resonances, Science Bulletin **65**, 373 (2020).

[26] J. Boulvert, T. Humbert, V. Romero-García, G. Gabard, E. R. Fotsing, A. Ross, J. Mardjono, and J.-P. Groby, Perfect, broadband, and sub-wavelength absorption with asymmetric

absorbers: Realization for duct acoustics with 3d printed porous resonators, Journal of Sound and Vibration **523**, 116687 (2022).

[27] S.-H. Seo, Y.-H. Kim, and K.-J. Kim, Design of silencer using resonator arrays with high sound pressure and grazing flow, Applied Acoustics **138**, 188 (2018).

[28] R. Ghaffarivardavagh, J. Nikolajczyk, S. Anderson, and X. Zhang, Ultra-open acoustic metamaterial silencer based on Fano-like interference, Physical Review B **99**, 024302 (2019).

[29] N. Jiménez, T. J. Cox, V. Romero-García, and J.-P. Groby, Metadiffusers: Deep-subwavelength sound diffusers, Scientific reports **7**, 1 (2017).

[30] E. Ballestero, N. Jimenez, J.-P. Groby, H. Aygun, S. Dance, and V. Romero-García, Metadiffusers for quasi-perfect and broadband sound diffusion, Applied Physics Letters **119**, 044101 (2021).

[31] R. V. Craster and S. Guenneau, *Acoustic metamaterials: Negative refraction, imaging, lensing and cloaking*, Vol. 166 (Springer Science & Business Media, 2012).

[32] P. A. Deymier, *Acoustic metamaterials and phononic crystals*, Vol. 173 (Springer Science & Business Media, 2013).

[33] W. S. Gan, *New acoustics based on metamaterials* (Springer, 2017).

[34] V. Romero-Garcia and A.-C. Hladky-Hennion, eds., *Fundamentals and applications of acoustic metamaterials: From seismic to radio frequency* (John Wiley & Sons, 2019).

[35] N. Jiménez, O. Umnova, and J.-P. Groby, eds., *Acoustic waves in periodic structures, metamaterials, and porous media: From fundamentals to industrial applications* (Springer, Cham, 2021).

[36] J. Allard and N. Atalla, *Propagation of sound in porous media: modelling sound absorbing materials*, 2nd ed. (John Wiley & Sons, 2009).

[37] L. E. Kinsler, A. R. Frey, A. B. Coppens, and J. V. Sanders, *Fundamentals of acoustics* (John wiley & sons, 2000).

[38] J. Blauert and P. Laws, Group delay distortions in electroacoustical systems, The Journal of the Acoustical Society of America **63**, 1478 (1978).

[39] A. Merkel, G. Theocharis, O. Richoux, V. Romero-García, and V. Pagneux, Control of acoustic absorption in one-dimensional scattering by resonant scatterers, Applied Physics Letters **107**, 244102 (2015).

[40] N. Jiménez, V. Romero-García, V. Pagneux, and J.-P. Groby, Quasiperfect absorption by subwavelength acoustic panels in transmission using accumulation of resonances due to slow sound, Phys. Rev. B **95**, 014205 (2017).

[41] V. Romero-García, N. Jiménez, J.-P. Groby, A. Merkel, V. Tournat, G. Theocharis, O. Richoux, and V. Pagneux, Perfect absorption in mirror-symmetric acoustic metascreens, Phys. Rev. Applied **14**, 054055 (2020).

[42] H. Y. Mak, X. Zhang, Z. Dong, S. Miura, T. Iwata, and P. Sheng, Going beyond the causal limit in acoustic absorption, Physical Review Applied **16**, 044062 (2021).

[43] G. F. Carrier, M. Krook, and C. E. Pearson, *Functions of a complex variable: theory and technique* (SIAM, 2005).

[44] M. Yang, C. Meng, C. Fu, Y. Li, Z. Yang, and P. Sheng, Subwavelength total acoustic absorption with degenerate resonators, Applied Physics Letters **107**, 104104 (2015).

[45] D. Lafarge, *Propagation du son dans les matériaux poreux à structure rigide saturés par un fluide viscothermique: définition de paramètres géométriques, analogie électromagnétique, temps de relaxation*, Ph.D. thesis, Université du Maine, Le Mans, France (1993).

[46] D. Lafarge, *Matériaux et Acoustique, I Propagation des Ondes Acoustiques*, edited by B. M. and P. C. (Lavoisier, Paris, 2006).

[47] J. Willis, Variational principles for dynamic problems for inhomogeneous elastic media, Wave Motion **3**, 1 (1981).

[48] A. Merkel, V. Romero-García, J.-P. Groby, J. Li, and J. Christensen, Unidirectional zero sonic reflection in passive $\mathcal{PT}$-symmetric willis media, Phys. Rev. B **98**, 201102 (2018).

[49] J.-P. Groby, M. Malléjac, A. Merkel, V. Romero-García, V. Tournat, D. Torrent, and J. Li, Analytical modeling of one-dimensional resonant asymmetric and reciprocal acoustic structures as Willis materials, New Journal of Physics **23**, 053020 (2021).

[50] M. J. Ablowitz, A. S. Fokas, and A. S. Fokas, *Complex variables: introduction and applications* (Cambridge University Press, 2003).

[51] M. Niskanen, J.-P. Groby, A. Duclos, O. Dazel, J. C. Le Roux, N. Poulain, T. Huttunen, and T. Lähivaara, Deterministic and statistical characterization of rigid frame porous materials from impedance tube measurements, The Journal of the Acoustical Society of America **142**, 2407 (2017).

[52] M. C. A. M. Peters, A. Hirschberg, A. J. Reijnen, and A. P. J. Wijnands, Damping and reflection coefficient measurements for an open pipe at low Mach and low Helmholtz numbers, Journal of Fluid Mechanics **256**, 499–534 (1993).

[53] D. L. Johnson, J. Koplik, and R. Dashen, Theory of dynamic permeability and tortuosity in fluid-saturated porous media, Journal of Fluid Mechanics **176**, 379–402 (1987).

[54] Y. Champoux and J. Allard, Dynamic tortuosity and bulk modulus in air-saturated porous media, Journal of Applied Physics **70**, 1975 (1991).

[55] D. Lafarge, P. Lemarinier, J. F. Allard, and V. Tarnow, Dynamic compressibility of air in porous structures at audible frequencies, The Journal of the Acoustical Society of America **102**, 1995 (1997).

[56] M. E. Delany and E. N. Bazley, Acoustical properties of fibrous absorbent materials, Applied acoustics **3**, 105 (1970).

[57] Z. Fellah, S. Berger, W. Lauriks, and C. Depollier, Verification of Kramers–Kronig relationship in porous materials having a rigid frame, Journal of Sound and Vibration **270**, 865 (2004).